2011

LQG/LTR control of induction motor

Girish Arvind Yajurvedi

Louisiana State University and Agricultural and Mechanical College, gyajur1@tigers.lsu.edu

LQG/LTR CONTROL OF INDUCTION MOTOR

A Thesis

Submitted to the Graduate Faculty of
Louisiana State University and
Agricultural and Mechanical College
in partial fulfillment of the
requirements for the Degree of
Master of Science in Electrical Engineering

in

the Department of Electrical and Computer Engineering

by
Girish Yajurvedi
Bachelor of Engineering, M. S. University, India. 2007.
December 2011

ACKNOWLEDGMENTS

I would like to sincerely thank my research advisor, Dr Guoxiang Gu for being a patient mentor over the course of my degree completion. His guidance and constant support helped me to stay motivated. I learnt a great deal from him about scientific writing and problem solving in the area of control system. I would also like to thank him for the financial support and the trust he had in me for undertaking this research endeavour. I couldn't have imagined having a better mentor for my masters thesis.

Apart from my major advisor i would also like to thank Dr Ernest Mendrela for providing the Power System Lab access for testing and design of drive. The wide range of equipments available in the lab helped a great deal in the hardware design progress. It was a great honour to have Dr Kemin Zhou and Dr Ernest Mendrela as committee member's for my masters thesis. I would like to thank them for their encouragement and suggestions regarding the thesis writing.

Finally I would like to thank my family for their unflinching support, without which my master studies would have been impossible.

TABLE OF CONTENTS

LIST OF FIGURES

ABSTRACT

Induction motors are the most rugged electrical equipment which are widely used in the industry. Owing to the non-linearity in its behaviour, it is not a trivial problem to solve and hence we are interested in using it as a control platform. Through several decades of research a wide number of control schemes have been developed for implementing the closed loop control. Based upon the merits and demerits of various schemes we choose a control scheme called the indirect vector control of Induction motor.

Using the electrical dynamics of the motor model we design a LQG/LTR controller. We employ a discretized model for the controller design. A step by step procedure has been outlined considering the two possible cases of minimum phase and non minimum phase systems.

Finally the speed tracking capability of the design is tested in $^{®}$Matlab $^{™}$Simulink using $^{®}$SimPowerSystem toolbox.

CHAPTER 1

INTRODUCTION

The primary motive of this thesis is to develop a simple and viable design procedure

for synthesis of multi-input/multi-out (MIMO) feedback control systems. A second motive

is validation of this design procedure by applying it to synthesis of the feedback controller

on an industrial grade $\frac{1}{2}$ H.P. induction motor that is implemented using a digital signal

processor (DSP) board.

Since 1960s, many different methods are developed to design MIMO feedback control

systems. Notable ones are linear quadratic Gaussian (LQG) and $\mathcal{H}_\infty$ control [5],[20]. There

are pros and cons for LQG and $\mathcal{H}_\infty$ based control design methods. Roughly speaking,

LQG control is aimed at minimizing the white noise disturbances. It has the advantages

of being easy to understand and simple to design. However it lacks robustness against

the modeling error of the MIMO system. A loop transfer recovery (LTR) procedure is

developed in the literature [10, 19] in conjunction with the linear quadratic regulator (LQR).

This LQR/LTR procedure aims to recover the loop transfer property achievable under the

state feedback. For continuous-time systems, LQR control admits infinity gain margin and

60° phase margin, and thus it is robust against the modeling uncertainty. However for

discrete-time systems, this approach is less effective. On the other hand $\mathcal{H}_\infty$ control is

rich in theory and more difficult to understand but admits robustness against unmodeled

dynamics. We will introduce loop shaping employed in $\mathcal{H}_\infty$ to LQR/LTR based design

method in hope that our new method retains the simplicity of the LQR/LTR meanwhile achieving the robustness against the modelling uncertainty.

1.1 Control of Induction Motors

Induction Motors is one of the most widely used and studied industrial equipment. It is well known that induction motor exhibits a nonlinear behaviour and the state variables of this multi variable system interact with each other to produce the output which is desired to be controlled. Induction motor drives can be broadly categorized in to types 1) Frequency-controlled drives and 2) Vector control drives. It is a general understanding that frequency controlled drives use the change in supply frequency as a means to control the speed of induction motor. Vector control is a method using which the dynamics of the Induction motor can be controlled in a manner similar to the separately excited DC motor. The principle reason for performing this transformation is that separately excited DC drives are simpler to control. "The flux in DC motors can be independently controlled, which when maintained constant contributes to the independent control of torque of the machine."[8] For implementing the vector control method, the angular position of the rotor flux is needed. There are two ways to implement vector control in a drive, a) Direct vector control and b) Indirect vector control which are based upon how the rotor flux angle is determined, through measurement or through calculation respectively. The performance of the vector control method depends on the accuracy of the parameters like L_r rotor inductance and R_r rotor resistance of induction motor and dynamically calculated flux and speed. In [17] concentration is on the estimation of the states for performance improvement. The motor model developed for the control problem is in reference to a frame rotating at synchronous

2

speed (ω_s). The contribution of [17] is that the load torque is included in system dynamics by choosing rotor speed ω_r as additional state. Since the dynamics of the model described takes into consideration the load torque, there is an improvement in the system response. The model used for the control purpose is similar to the one we adopted, except for the inclusion of rotor speed dynamics. Since in our design we propose to use optimal feedback control method for the current dynamics of the motor we hope to compensate the load torque changes. A DSP is used to implement the controller and estimator in [17] and designing is carried out in discrete time.

In implementing vector control, there is a scheme that takes into consideration the estimated speed rather than measured speed, as used in [7]. By doing so the need for speed measuring sensor can be eliminated, if sufficiently accurate estimation can be guaranteed. Consequently a motor model consisting of rotor speed as one of its state is constructed and extended Kalman filter is applied. The emphasis has been given to the estimation in [7]. The results of motor speed estimation are assured, but an increased order plant model requires a higher processing speed. Hence a floating point DSP is used to implement the controller and the designing is carried out in discrete time. A somewhat similar implementation has been adopted in [14], wherein LQR is designed along with the a Lyapunov filter. In [14] the plant uncertainty has been taken into account for a robust performance, citing the nonlinear behaviour of thyristors, unmodelled dynamics of the actuators, and variation of the inductance while near saturation as some of the reasons for uncertainties. Weighting matrices have been designed using the loop shaping procedure. The model used is a reduced order SISO model, and the designing is carried out in continuous time. It does not consider the analysis of non-minimum phase plants which is a major factor since sampling

can result in non-minimum phase plants, even though continuous time plant is minimum phase.

Because the motor model is nonlinear, nonlinear control method has also been tested as shown in [15], wherein field oriented control is applied using a ™DSPACE with TMS320C30 floating point controller. The approach chosen is input output linearisation technique for the controller design. The actual design of controller is carried out in continuous time and using discretization for the final controller. The estimation part is implemented by Kalman filtering which is designed in discrete time. As the controller is continuous in time but implementation is in discrete time, several factors such as time delay have to be considered. In [18] and [2], LQR and H_2 control methods have been implemented on continuous-time and discrete-time models respectively. There is a slight variation in how the implementation of the control is carried out in this thesis. We consider loop shaping methodology for performance improvement. As done in [2], we will consider actuator saturation while testing the design in simulation by using a simple simulink saturation block.

Considering the pros and cons of the existing design methods discussed above, an attempt has been made to provide the MIMO controller design perspective for discrete-time systems. For tackling the problem of accurate estimation, we use the theory of asymptotic recovery to design an estimator to assure perfect recovery for minimum phase plants. Since the plant parameters are obtained using off-line tests and the model does not consider the various thermal effect on the plant parameters, it is imperative that the designed controller has good disturbance rejection and gain stability margin. In light of [3], a robust performance of the closed loop system can be achieved if appropriate loop shaping is performed.

1.2 Thesis Overview

Chapter2 Motor Modelling: This chapter starts with the reason and benefits of implementing D-Q (3ph to 2ph) transformation of the induction motor model. Following the D-Q transformation, all the three phase electrical circuit parameters, like M.M.F, current, magnetizing current, flux linkage and voltages, are expressed in D-Q terms. Finally the transformed stator and rotor voltage equations are constructed in a general rotating reference frame. The reason for constructing the voltage equations in general reference frame is that the principle of the vector control method can be applied. Roughly speaking, when the voltage and current quantities are expressed in a reference frame rotating along with the rotor flux linkage phasor, the control of induction motor becomes similar to that of a separately excited DC motor. Finally a two input two output induction motor state space model is provided that is used in later chapters for the design of the feedback controller.

Chapter3 MIMO control design: Initially the various control methods for SISO systems are discussed. The notion of smallness of a transfer function is explained with respect to the singular values of the frequency response of the system. Consequently as mentioned in [3], arguments are given to extend the frequency based control methods to MIMO system. A mathematical result is introduced which states that for a stabilizable and detectable plant, the frequency shapes of the closed loop sensitivity and complementary sensitivity are the same as that of the left and right coprime factors of open loop plant, respectively. This fact allows us to shape the plant for desired loop shape and then carry out the LQR control solution. A result from [10] is used to construct the observer solution and to achieve perfect recovery for a minimum phase plant. We use a theorem from [19] to come up with an er-

ror function which will help to quantify the recovery error achieved for the non-minimum phase plants. In [19], a procedure to factor out the non-minimum phase zeros of the plant has been derived so that the remaining minimum phase system can be used for the design of the observer gain. This method is less effective due to the use of the transfer matrix for factorizing the non-minimum phase zeros of the plant. A simpler method is from [6] that provides the state-space formulas to arrive at the desired factorization.

Chapter4 Simulation and DSP: In this chapter the linearization of the plant is carried out and selection of weighting function to meet the performance requirements. The weighted plant is then used to design LQG solution, and closed loop frequency response and step is shown. The implementation of the controller in two degree of freedom and in actual Field oriented control methodology. Finally details about the hardware equipment used for the controller implementation is explained along with software implementation and ™TI Digital motor control library and IQmath library.

Chapter5 Conclusion and further prospects of work.

CHAPTER 2

DYNAMICAL MODELLING OF INDUCTION MOTOR

Consider a 3-phase 2 pole induction motor having N_s and N_r as effective winding number of turns in stator and rotor respectively, we assume that the air gap is uniform and stator and rotor windings are sinusoidally distributed. The rotor windings are short circuited and the stator is connected to a balanced 3-phase voltage source. As mentioned in [12] when a 3-phase balanced voltage is applied to the stator, its windings produce magneto motive force (M.M.F.) in the air gap which rotates at the angular speed equal to the frequency of the power supply (ω_s). If the speed of the rotor is different from ω_s, the rotating M.M.F. will induce a current i_r in the short circuited rotor, which in turn induces the dynamic motion of the induction motor. The frequency of the rotor current i_r depends on the difference between ω_s and rotor speed ω_r. For the purpose of control, we will describe the dynamics of the induction motor in the form of state-space equations.

An induction motor has six voltage equations, three of which for stator and the other three for rotor. As a result, the dynamic order of the the induction motor model is six. By using the D-Q transformation method [12] for induction motors, we can express the 3-phase current, flux linkage, and voltage quantities in 2-phases D and Q, i.e., the direct and quadrature components. Such a D-Q transformation reduces the complexity of the mathematical model, while retaining all the essential equations for the dynamics of the system.

Associate each phase of A, B, C with the flux linkages ψ_{sA}, ψ_{sB}, and ψ_{sC}, respectively. The per phase voltage in stator and rotor can be described by

$$u_{sA}(t) = R_s i_{sA}(t) + \frac{d\psi_{sA}}{dt},$$

$$u_{sB}(t) = R_s i_{sB}(t) + \frac{d\psi_{sB}}{dt}, \tag{2.1}$$

$$u_{sC}(t) = R_s i_{sC}(t) + \frac{d\psi_{sC}}{dt},$$

where $u_{sA}(t), u_{sB}(t)$ and $u_{sC}(t), i_{sA}(t), i_{sB}(t)$ and $i_{sC}(t)$ are the instantaneous values of the stator phase voltages and currents, respectively. Similar expressions for the rotor circuit are

$$u_{ra}(t) = R_r i_{ra}(t) + \frac{d\psi_{ra}}{dt},$$

$$u_{rb}(t) = R_r i_{rb}(t) + \frac{d\psi_{rb}}{dt}, \tag{2.2}$$

$$u_{rc}(t) = R_r i_{rc}(t) + \frac{d\psi_{rc}}{dt},$$

where $u_{ra}(t), u_{rb}(t)$ and $u_{rb}(t), i_{ra}(t), i_{rb}(t)$ and $i_{rc}(t)$ are the instantaneous values of the rotor phase voltages and currents, respectively. Again ψ_{ra}, ψ_{rb} and ψ_{rc} are the flux linkages associated with each phase in rotor. The flux linkages in individual phase stators are expressed as follows:

$$\psi_{sA} = \bar{L}_s i_{sA} + \bar{M}_s i_{sB} + \bar{M}_s i_{sC} + \bar{M}_{sr} \cos(\theta_r) i_{ra}$$

$$+ \bar{M}_{sr} \cos\left(\theta_r + \frac{2\pi}{3}\right) i_{rb} + \bar{M}_{sr} \cos\left(\theta_r + \frac{4\pi}{3}\right) i_{rc},$$

$$\psi_{sB} = \bar{L}_s i_{sB} + \bar{M}_s i_{sA} + \bar{M}_s i_{sC} + \bar{M}_{sr} \cos(\theta_r) i_{rb}$$

$$+ \bar{M}_{sr} \cos\left(\theta_r + \frac{2\pi}{3}\right) i_{rc} + \bar{M}_{sr} \cos\left(\theta_r + \frac{4\pi}{3}\right) i_{ra}, \qquad (2.3)$$

$$\psi_{sC} = \bar{L}_s i_{sC} + \bar{M}_s i_{sB} + \bar{M}_s i_{sA} + \bar{M}_{sr} \cos(\theta_r) i_{rc}$$

$$+ \bar{M}_{sr} \cos\left(\theta_r + \frac{2\pi}{3}\right) i_{ra} + \bar{M}_{sr} \cos\left(\theta_r + \frac{4\pi}{3}\right) i_{rb}.$$

In above equations, $\bar{L}_s$ is the self inductance of stator phase winding, $\bar{M}_s$ is the mutual inductance between the stator windings, θ_r is the rotor angle and $\bar{M}_{sr}$ is the maximal value of the stator-rotor mutual inductance. The rotor flux linkages for three individual phases are

$$\psi_{ra} = \bar{L}_r i_{ra} + \bar{M}_r i_{rb} + \bar{M}_r i_{rc} + \bar{M}_{sr} \cos(\theta_r) i_{sA}$$

$$+ \bar{M}_{sr} \cos\left(\theta_r + \frac{4\pi}{3}\right) i_{sB} + \bar{M}_{sr} \cos\left(\theta_r + \frac{2\pi}{3}\right) i_{sC},$$

$$\psi_{rb} = \bar{L}_r i_{rb} + \bar{M}_r i_{ra} + \bar{M}_r i_{rc} + \bar{M}_{sr} \cos\left(\theta_r + \frac{2\pi}{3}\right) i_{sA} \qquad (2.4)$$

$$+ \bar{M}_{sr} \cos\left(\theta_r\right) i_{sB} + \bar{M}_{sr} \cos\left(\theta_r + \frac{4\pi}{3}\right) i_{sC},$$

$$\psi_{rc} = \bar{L}_r i_{rc} + \bar{M}_r i_{ra} + \bar{M}_r i_{rb} + \bar{M}_{sr} \cos\left(\theta_r + \frac{4\pi}{3}\right) i_{sA}$$

$$+ \bar{M}_{sr} \cos\left(\theta_r + \frac{2\pi}{3}\right) i_{sB} + \bar{M}_{sr} \cos(\theta_r) i_{sC}.$$

where $\bar{L}_r$ is the self-inductance of rotor winding, $\bar{M}_r$ is the mutual inductance between two rotor phases. The six equations in (2.1) and (2.2) are arranged in the matrix form using

9

equations (2.3) and (2.4).For convenience denote

$$\mathbf{u}_s = \begin{bmatrix} u_{sA} \\ u_{sB} \\ u_{sC} \end{bmatrix}, \quad \mathbf{u}_r = \begin{bmatrix} u_{ra} \\ u_{rb} \\ u_{rc} \end{bmatrix}, \quad \mathbf{i}_s = \begin{bmatrix} i_{sA} \\ i_{sB} \\ i_{sC} \end{bmatrix}, \quad \mathbf{i}_r = \begin{bmatrix} i_{ra} \\ i_{rb} \\ i_{rc} \end{bmatrix}. \quad (2.5)$$

as vector valued voltages and currents in stator and rotor, respectively. Let s be the Laplace

variable that stands for differential operator in time domain. Define the following matrices

$$Z_{ss}(s) = \begin{bmatrix} R_s + s\bar{L}_s & s\bar{M}_s & s\bar{M}_s \\ s\bar{M}_s & R_s + s\bar{L}_s & s\bar{M}_s \\ s\bar{M}_s & s\bar{M}_s & R_s + s\bar{L}_s \end{bmatrix}, \quad (2.6)$$

$$Z_{sr}(s) = \begin{bmatrix} p\bar{M}_{sr}\cos\theta & s\bar{M}_{sr}\cos\theta_1 & s\bar{M}_{sr}\cos\theta_2 \\ s\bar{M}_{sr}\cos\theta_2 & s\bar{M}_{sr}\cos\theta & s\bar{M}_{sr}\cos\theta_1 \\ s\bar{M}_{sr}\cos\theta_1 & s\bar{M}_{sr}\cos\theta_2 & s\bar{M}_{sr}\cos\theta \end{bmatrix}, \quad (2.7)$$

$$Z_{rs}(s) = \begin{bmatrix} s\bar{M}_{sr}\cos\theta & s\bar{M}_{sr}\cos\theta_2 & s\bar{M}_{sr}\cos\theta_1 \\ s\bar{M}_{sr}\cos\theta_1 & s\bar{M}_{sr}\cos\theta & s\bar{M}_{sr}\cos\theta_2 \\ s\bar{M}_{sr}\cos\theta_2 & s\bar{M}_{sr}\cos\theta_1 & s\bar{M}_{sr}\cos\theta \end{bmatrix}, \quad (2.8)$$

$$Z_{rr}(s) = \begin{bmatrix} R_r + s\bar{L}_r & s\bar{M}_r & s\bar{M}_r \\ s\bar{M}_r & R_r + ps\bar{L}_r & s\bar{M}_r \\ s\bar{M}_r & s\bar{M}_r & R_r + s\bar{L}_r \end{bmatrix}, \quad (2.9)$$

10

where $\theta = \theta_r, \theta_1 = \theta_r + \frac{2\pi}{3}, \theta_2 = \theta_r + \frac{4\pi}{3}$. With $U_s(s)$, $U_r(s)$, $I_s(s)$ and $I_r(s)$ as Laplace transforms of $\mathbf{u}_s$, $\mathbf{u}_r$, $\mathbf{i}_s$ and $\mathbf{i}_r$, respectively, the dynamic equations in (2.1) and (2.2) can now be described in Laplace domain by

$$
\begin{bmatrix} U_s \\ U_r \end{bmatrix} = \begin{bmatrix} Z_{ss}(s) & Z_{sr}(s) \\ Z_{rs}(s) & Z_{rr}(s) \end{bmatrix} \begin{bmatrix} I_s \\ I_r \end{bmatrix}. \tag{2.10}
$$

In order to obtain the state space equation for the dynamic model in (2.1) and (2.2), which are now described equivalently by (2.10) in Laplace domain, we take the derivatives of the currents as the state variables. Since the currents in each stator phases can be measured, they are taken as the output of the state space system. The control inputs will be specified later. Prior to deriving the state equations, D-Q transformation is applied first to the stator and rotor voltage equations in (2.1) and (2.2). The first step is to describe the space phasor forms for three phase currents, voltages and flux linkages one by one. These phasor forms will then be used in (2.1) and (2.2). Finally the transformed stator and rotor voltages will be used to arrive at the transformed model for (2.10).

For simplicity, we make the following assumptions [16] (page-6) in modelling the induction motor:

- A smooth air gap 3-phase machine is considered with symmetrical two-poles.

- The effects of slotting are neglected.

- The permeability of the iron parts is assumed to be infinite and the flux density is considered radial in air-gap.

- The effects due to iron loss are neglected

In the next several sections, the space phasor analysis will be carried out for stator and rotor currents, magnetizing currents, flux linkages and voltages.

2.1 Stator and Rotor Current and M.M.F. Space Phasors.

For a balanced 3-phase stator circuit at any given arbitrary time, the currents in three different phases are $i_{sA}(t)$, $i_{sB}(t)$ and $i_{sC}(t)$ respectively. Since the neutral of the system is isolated, there is no zero sequence current in the system. Hence the following relation

$$i_{sA}(t) + i_{sB}(t) + i_{sC}(t) = 0 \qquad (2.11)$$

holds. Let N_s be the effective number of turns in the stator windings. Figure 2.1 provides a schematic for the three phase induction motor.
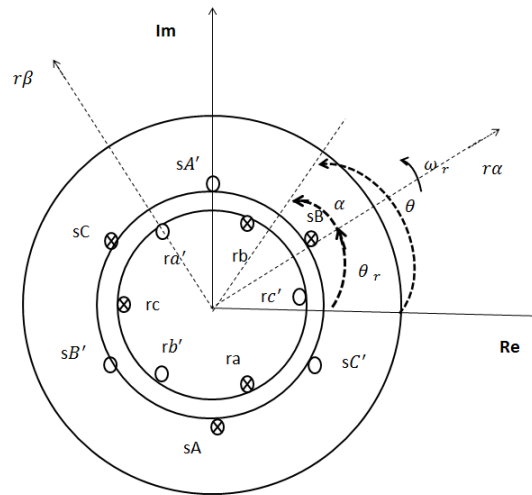
Figure 2.1

Cross-section of an elementary symmetrical three-phase machine [16] (p-6)

In Figure 2.1,

- **Re** and **Im** are the real and imaginary axis fixed to the stator frame (these axis also coincide with the sD and sQ axis defined later)

- $r\alpha$-$r\beta$ is the rotating reference frame fixed to the rotor, speed of rotation of this frame with respect to **Re and Im** is ω_r.

- "θ is the angle around the periphery with reference to the axis of the stator windings sA, which represents the angular position of the stator flux linkage."-[16](page-7)

- "α is the angle around the periphery with respect to the axis of the rotor winding ra."[16] (page-7)

For Figure 2.1, the resultant M.M.F. distribution $f_s(\theta, t)$ produced by the stator windings is given by

$$f_s(\theta, t) = N_s[i_{sA}(t)\cos(\theta) + i_{sB}(t)\cos(\theta - 2\pi/3) + i_{sC}(t)\cos(\theta - 4\pi/3)]. \qquad (2.12)$$

Using complex notation, we can rewrite the above equation as:

$$f_s(\theta, t) = \frac{3}{2}N_s\text{Re}\left[\frac{2}{3}(i_{sA}(t) + ai_{sB}(t) + a^2 i_{sC}(t))e^{-j\theta}\right] \qquad (2.13)$$

Rewriting flux linkage as:

$$f_s(\theta, t) = \frac{3}{2}N_s\text{Re}\left[\bar{i}_s(t)e^{-j\theta}\right]. \qquad (2.14)$$

Then it can be verified that

$$\bar{i}_s(t) = \frac{2}{3}[i_{sA}(t) + ai_{sB}(t) + a^2 i_{sC}(t)] = |\bar{i}_s|e^{j\alpha_s} \tag{2.15}$$

where $a = e^{\frac{j2\pi}{3}}$ is a spatial operator, "$|\bar{i}_s|$ is modulus of stator space phasor current, and α_s is the phase angle with respect to the real axis fixed to the stator. The real axis of the stator is designated as the **Direct** axis and the imaginary axis as **Quadrature** axis. Both the modulus and the phase angle of the stator current space phasor are dependent on time. Since in practice the spatial displacement and instantaneous magnitude of peak of the sinusoidal stator M.M.F. space phasor are determined by the space phasor of the stator current, the description of space phasor of stator M.M.F. can be expressed by"[16] (page-7)

$$\bar{f}_s(t) = N_s \bar{i}_s(t) = \bar{f}_{sA}(t) + \bar{f}_{sB}(t) + \bar{f}_{sC}(t). \tag{2.16}$$

Also from (2.15), stator current space phasor can be expressed in terms of space phasor of three phases as

$$\bar{i}_s = \bar{\mathbf{i}}_{sA} + \bar{\mathbf{i}}_{sB} + \bar{\mathbf{i}}_{sC}. \tag{2.17}$$

where $\bar{\mathbf{i}}_{sA} = i_{sA}(t), \bar{\mathbf{i}}_{sB} = ai_{sB}(t)$ and $\bar{\mathbf{i}}_{sC} = a^2 i_{sC}(t)$. To further the space phase analysis using the two axis property, $\bar{i}_s(t)$ from (2.15) can be written as

$$\bar{i}_s = i_{sD}(t) + ji_{sQ}(t). \tag{2.18}$$

14

In a symmetrical 3-ph machines, the direct and quadrature-axis stator currents $i_{sD}(t)$ and $i_{sQ}(t)$ are imaginary quadrature phase current components respectively, which are expressed as

$$i_{sD}(t) = c[i_{sA}(t) - \frac{1}{2}i_{sB}(t) - \frac{1}{2}i_{sC}(t)],$$

$$i_{sQ}(t) = c\frac{\sqrt{3}}{2}[i_{sB}(t) - i_{sC}(t)],$$

$$i_{sD}(t) = \text{Re}(\bar{i}_s(t)) = \text{Re}\left[\frac{2}{3}(i_{sA}(t) + ai_{sB}(t) + a^2 i_{sC}(t))\right], \qquad (2.19)$$

$$i_{sQ}(t) = \text{Im}(\bar{i}_s(t)), = \text{Im}\left[\frac{2}{3}(i_{sA}(t) + ai_{sB}(t) + a^2 i_{sC}(t))\right].$$

where $c = \frac{2}{3}$ is a constant. We can also obtain the corresponding instantaneous value of the phase variables by taking the projections of the space phasor quantity on the corresponding phase axis as explained in Figure 2.2:

$$\text{Re}(\bar{i}_s(t)) = \text{Re}\left[\frac{2}{3}(i_{sA}(t) + ai_{sB}(t) + a^2 i_{sC}(t))\right]$$

$$= \frac{2}{3}[i_{sA}(t) - \frac{1}{2}i_{sB}(t) - \frac{1}{2}i_{sC}(t)] = i_{sA}(t),$$

$$\text{Re}(a^2\bar{i}_s(t)) = \text{Re}\left[\frac{2}{3}(a^2 i_{sA}(t) + i_{sB}(t) + ai_{sC}(t))\right] = i_{sB}(t), \qquad (2.20)$$

$$\text{Re}(a\bar{i}_s(t)) = \text{Re}\left[\frac{2}{3}(ai_{sA}(t) + a^2 i_{sB}(t) + i_{sC}(t))\right] = i_{sC}(t).$$

Similar set of relations can be developed for the rotor M.M.F. and current components. Consider that the equivalent number of rotor winding is N_r. The rotor flux linkage is
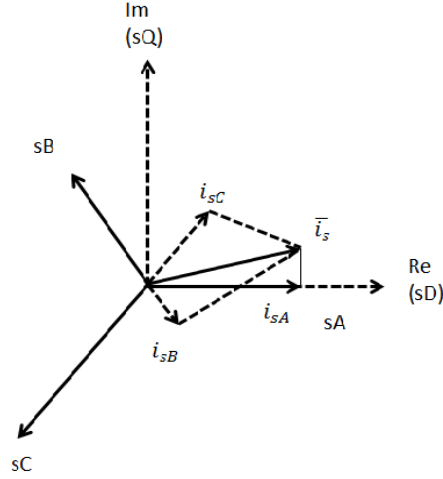
Figure 2.2

projection of stator current space phasor [16](p-10)

expressed as follows:

$$f_r(\theta, t) = N_r[i_{rA}(t)\cos(\alpha) + i_{rB}(t)\cos(\alpha - 2\pi/3) + i_{rC}(t)\cos(\alpha - 4\pi/3)]$$

$$= \frac{3}{2}N_r\mathrm{Re}\left[\frac{2}{3}(i_{rA}(t) + ai_{sB}(t) + a^2 i_{rC}(t))e^{-j\alpha}\right]. \tag{2.21}$$

From the above equation, the rotor current space phasor can be obtained as:

$$\bar{i}_r(t) = \frac{2}{3}[i_{rA}(t) + ai_{rB}(t) + a^2 i_{rC}(t)] = |\bar{i}_r|e^{j\alpha_r},$$

$$\bar{i}_r(t) = i_{r\alpha}(t) + ji_{r\beta}(t). \tag{2.22}$$

where α_r is the phase angle of the rotor current phasor with respect to the axis $r\alpha$. While in

(2.15) the stator current space phasor is expressed in reference to the stationary reference

16

Re and **Im**, we can also express the stator current space phasor with respect to the rotor reference frame $r\alpha\text{-}r\beta$ ($\bar{i}'_s$) as follows:

$$\bar{i}'_s = \bar{i}_s e^{-j\theta_r},$$

$$\bar{i}_s = \bar{i}'_s e^{j\theta_r}, \tag{2.23}$$

$$\bar{i}_s = i_{sD} + j i_{sQ},$$

$$\bar{i}'_s = i_{sd} + j i_{sq}.$$

We have the expression of the rotor current phasor with respect to the rotating reference frame in equation (2.22,2.21), which can be expressed in θ and θ_r. By Figure 2.1, replacing α in 2.21 with $\theta - \theta_r$ yields

$$f_r(\theta, \theta_r, t) = \frac{3}{2} N_r \mathrm{Re}\big[\bar{i}_r e^{-i(\theta - \theta_r)}\big] = \frac{3}{2}\mathrm{Re}(\bar{i}'_r e^{-j\theta}),$$

$$\bar{i}'_r = \bar{i}_r e^{\theta_r} = |\bar{i}_r| e^{j(\alpha_r + \theta_r)} = |\bar{i}_r| e^{j\alpha'_r} \tag{2.24}$$

$$\bar{i}'_r = i_{rd} + j i_{rq}$$

where $\bar{i}'_r$ is the space phasor of rotor current expressed in the stationary reference frame which is evident from the Figure 2.3. In relation to the reference frame that is fixed to the stator (referred as sD and sQ), the reference frame fixed to the rotor rotates at an angular speed ω_r. Hence at any give time angle between the two reference frames is θ_r.

The resultant M.M.F. in the motor circuit can be expressed as

$$f(\theta, \theta_r, t) = f_s(\theta, t) + f_r(\theta, \theta_r, t). \tag{2.25}$$

17
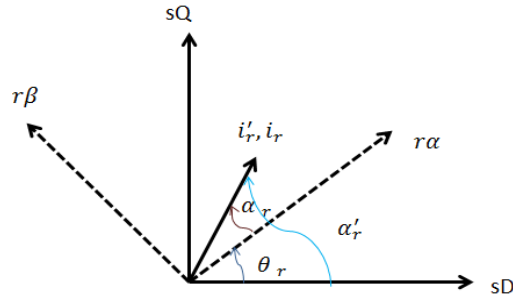
Figure 2.3

Relation between stationary and rotating reference frames [16](p-12)

Using the flux linkages of stator and rotor from the previous part, we obtain

$$f(\theta, \theta_r, t) = \frac{3}{2} N_s [\mathrm{Re}(\bar{i}_s e^{-j\theta}) + \frac{N_r}{N_s} \mathrm{Re}(\bar{i}'_r e^{-j\theta})],$$

$$= \frac{3}{2} \mathrm{Re} \left[(\bar{i}_s + \frac{N_r}{N_s} \bar{i}'_r) e^{-j\theta} \right]. \tag{2.26}$$

which contains the current part $\bar{i}_m = (\bar{i}_s + \frac{N_r}{N_s} \bar{i}'_r) e^{-j\theta}$ called the magnetizing current space phasor expressed in the stationary reference frame fixed to stator.

2.2   Flux Linkages and Stator-Rotor Voltages in Space Phasor

In a stationary reference frame fixed (**Re-Im**) to the stator, the total flux-linkage space phasor for stator winding is expressed as

$$f(\theta, \theta_r, t) = \frac{3}{2} \psi_s = \frac{2}{3} (\psi_{sA} + a\psi_{sB} + a^2 \psi_{sc}).$$

18

where the instantaneous values of space phasor flux linkages are expressed as shown in (2.3). By substituting equations (2.3), (2.15), and (2.24) into (2.27), we obtain the stator flux linkage with respect to the stationary reference frame fixed to the stator as follows:

$$\bar{\psi}_s = L_s \bar{i}_s + L_m \bar{i}'_r \qquad (2.27)$$

where $L_s = \bar{L}_s - \bar{M}_s$ is the total three-phase stator inductance and $L_m = \frac{3}{2}\bar{M}_{sr}$ is three phase magnetizing inductance. The two flux linkage components in above equations are self flux linkage space phasor of stator phase caused by the stator current and mutual flux linkage space phasor due to rotor current ($\bar{i}'_r$ is expressed in stationary reference)[16](page14). The stator flux linkage can be defined in terms of the direct and quadrature axis flux linkage components as follows:

$$\bar{\psi}_s = \psi_{sD} + j\psi_{sQ} \qquad (2.28)$$

where $\psi_{sD} = L_s i_{sD} + L_m i_{rd}$ is the direct component and $\psi_{sQ} = L_s i_{sQ} + L_m i_{rQ}$ is the quadrature component. In above equations i_{sD}, i_{sQ} and i_{rd}, i_{rq} are the instantaneous values of the direct and quadrature axis stator and rotor currents, respectively, as expressed in equations (2.23) and (2.24).

To develop the space phasor for the flux linkage of the rotor in the reference frame $r\alpha - r\beta$, we use the following expression:

$$\bar{\psi}_r = \frac{2}{3}[\psi_{ra}(t) + a\psi_{rb}(t) + a^2\psi_{rc}(t)] \qquad (2.29)$$

19

where $\psi_{ra}(t)$, $\psi_{rb}(t)$ and $\psi_{rc}(t)$ are the instantaneous values of the rotor flux linkages in rotor phases ra, rb, and rc, respectively as expressed in equation (2.4). Using the expressions (2.4), (2.22), (2.15), and (2.23), the space phasor for rotor flux is obtained as

$$\bar{\psi}_r = L_r \bar{i}_r + L_m \bar{i}'_s \tag{2.30}$$

where $L_r = \bar{L}_r - \bar{M}_r$ is the total three-phase rotor inductance and $\bar{i}'_s$ is the space phasor of the stator current expressed in the reference frame fixed to the rotor. We explain two terms in the above equation as stated in [16] (page-16) as follows: a) $L_r \bar{i}_r$ is the rotor self inductance expressed in the reference frame fixed to the rotor and is primarily because of rotor current; b) $L_m \bar{i}'_s$ is the mutual flux-linkage space phasor produced by the stator currents and expressed in the same rotor reference frame. The rotor flux linkage can be expressed in the form of two axis component as

$$\bar{\psi}_r = \psi_{r\alpha} + j\psi_{r\beta}. \tag{2.31}$$

where $\psi_{r\alpha} = L_r i_{r\alpha} + L_m i_{sd}$ and $\psi_{r\beta} = L_r i_{r\beta} + L_m i_{sq}$ and the current components $i_{r\alpha}, i_{sd}, i_{r\beta}$ and i_{sq} are direct and quadrature current components expressed with reference to the frame fixed to the rotor. As described in equation (2.24) , the rotor flux linkage is expressed in stationary reference frame fixed to stator by using the transformation $e^{j\theta_r}$ as next:

$$\bar{\psi}_r{}' = \psi_{rd} + j\psi_{rq} = \bar{\psi}_r e^{j\theta_r}, \tag{2.32}$$

$$\bar{\psi}_r{}' = (L_r \bar{i}_r' + L_m \bar{i}_s' e^{j\theta_r}) = L_r \bar{i}_r' + L_m \bar{i}_s. \tag{}$$

Voltage space phasor can be expressed principally in a manner similar to the current space phasors. With respect to the stationary reference frame, stator voltage space phasors are given by

$$\bar{u}_s = \frac{2}{3}[u_{sA}(t) + a u_{sB}(t) + a^2 u_{sC}(t)] = u_{sD} + j u_{sQ}. \tag{2.33}$$

We first provide the expression for the rotor voltage space phasor in reference frame fixed to the rotor:

$$\bar{u}_r = \frac{2}{3}[u_{ra}(t) + a u_{rb}(t) + a^2 u_{rc}(t)] = u_{r\alpha} + j u_{r\beta}. \tag{2.34}$$

The relation between three phase quantities and the quadrature phase quantities follows the same analogy as in the case of the rotor current space phasor. We can now convert the rotor voltage space phasor in the reference frame fixed to the stator by using the following relation:

$$\bar{u}_r{}' = \bar{u}_r e^{j\theta_r} = u_{rd} + j u_{rq}. \tag{2.35}$$

2.3   Voltage Equations in a General Reference Frame

For the stator and rotor space phasors of current, voltage, and flux linkage we have two versions one in the stationary reference frame fixed to the stator, and the other in the rotor reference frame rotating at the speed ω_r. In this section we develop the stator and rotor voltage equations in a general reference frame rotating at speed ω_g. The benefit for doing so is that we can easily change the expressions from stator and rotor reference to any other arbi-

trary reference frame as required simply by selecting suitable ω_g. In previous sections, $\bar{i}_s$ and i_r' are the stator and rotor space phasors expressed in stator reference frame. See equations (2.15) and (2.24). Now consider a general reference frame with direct and quadrature reference frames x and y respectively rotating at a speed $\omega_g = \frac{d\theta_g}{dt}$ as explained in Figure 2.4. Using the same analogy as used in equation (2.23) to change the reference from fixed to a reference frame rotating at the speed ω_r, we can deduce following relationships.
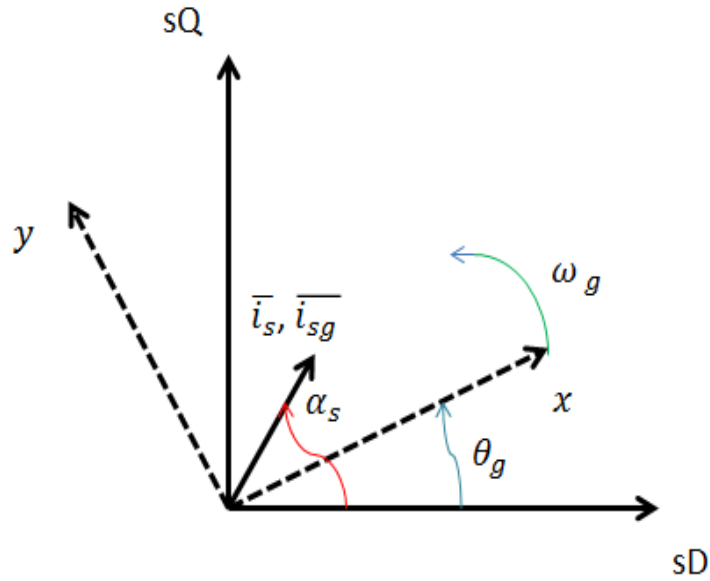
Figure 2.4

Stator space phasor quantities in general reference frame [16](p-38)

$$\bar{i}_{sg} = \bar{i}_s e^{-j\theta_g} = i_{sx} + j i_{sy} \tag{2.36}$$

$$u_{sg} = \bar{u}_s e^{-j\theta_g} = u_{sx} + ju_{sy} \tag{2.37}$$

$$\bar{\psi}_{sg} = \bar{\psi}_s e^{-j\theta_g} = \psi_{sx} + j\psi_{sy} \tag{2.38}$$

By Figure 2.5 next explains the positioning of rotor space phasor with respect to the general reference frame. From Figure 2.5, it is clear that the angle between the real axis (x) and the
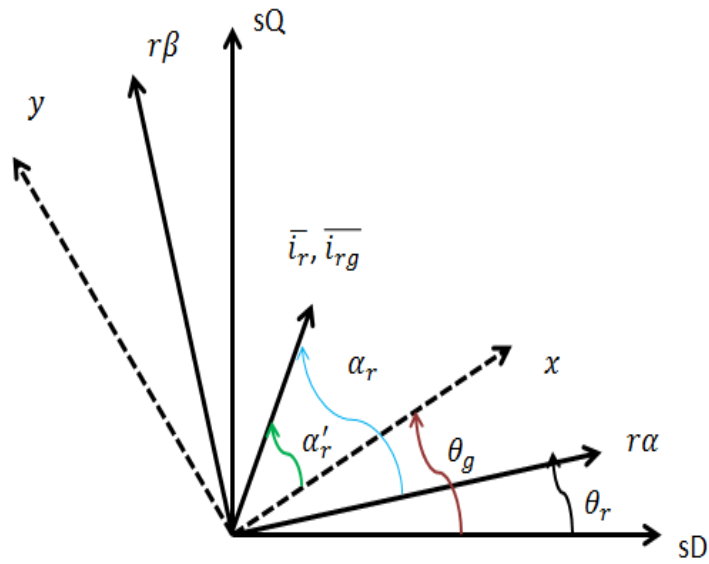
Figure 2.5

Rotor phasor quantities in general reference frame [16](p-39)

reference frame rotating with rotor ($r\alpha$) is $\theta_g - \theta_r$ [16](page-39). Hence we can obtain the following relationships for the rotor components:

$$\bar{i}_{rg} = |\bar{i}_r|e^{j\alpha_r}e^{-j(\theta_g - \theta_r)} = \bar{i}_r e^{-j(\theta_g - \theta_r)} = i_{rx} + ji_{ry}, \tag{2.39}$$

$$\bar{u}_{rg} = \bar{u}_r e^{-j(\theta_g - \theta_r)} = u_{rx} + ju_{ry}, \tag{2.40}$$

$$\bar{\psi}_{rg} = \bar{\psi}_r e^{-j(\theta_g - \theta_r)} = \psi_{rx} + j\psi_{ry}. \tag{2.41}$$

The voltage equations using space phasor quantities in induction motor stator and rotor are given by

$$\bar{u}_{sg} = R_s \bar{i}_{sg} + \frac{d\bar{\psi}_{sg}}{dt} + j\omega_g \bar{\psi}_{sg}, \tag{2.42}$$

$$\bar{u}_{rg} = R_r \bar{i}_{rg} + \frac{d\bar{\psi}_{rg}}{dt} + j(\omega_g - \omega_r)\bar{\psi}_{rg}, \tag{2.43}$$

$$\bar{\psi}_{sg} = L_s \bar{i}_{sg} + L_m \bar{i}_{rg}, \tag{2.44}$$

$$\bar{\psi}_{rg} = L_r \bar{i}_{rg} + L_m \bar{i}_{sg}. \tag{2.45}$$

So the final voltage equations are obtained as

$$\bar{u}_{sg} = R_s \bar{i}_{sg} + \frac{d(L_s \bar{i}_{sg})}{dt} + \frac{d(L_m \bar{i}_{rg})}{dt} + j\omega_g (L_s \bar{i}_{sg} + L_m \bar{i}_{rg}), \tag{2.46}$$

$$\bar{u}_{rg} = R_r \bar{i}_{rg} + \frac{d(L_r \bar{i}_{rg})}{dt} + \frac{d(L_m \bar{i}_{sg})}{dt} + j(\omega_g - \omega_r)(L_r \bar{i}_{rg} + L_m \bar{i}_{sg}). \tag{2.47}$$

Hence the dynamic equation in (2.10) is now transformed into

$$
\begin{bmatrix} u_{sx} \\ u_{sy} \\ u_{rx} \\ u_{ry} \end{bmatrix} = \begin{bmatrix} R_s + sL_s & -\omega_g L_s & sL_m & -\omega_g L_m \\ \omega_g L_s & R_s + sL_s & \omega_g L_m & pL_m \\ sL_m & -(\omega_g - \omega_r)L_m & R_r + sL_r & -(\omega_g - \omega_r)L_r \\ (\omega_g - \omega_r)L_m & sL_m & (\omega_g - \omega_r)L_r & R_r + sL_r \end{bmatrix}
\begin{bmatrix} i_{sx} \\ i_{sy} \\ i_{rx} \\ i_{ry} \end{bmatrix}
\tag{2.48}
$$

where s is the Laplace variable, and is derivative operator in time domain. Now if we consider the set of equations in a stationary reference frame, i.e., $\omega_g = 0$, we obtain the following quadrature pulse model as mentioned in [16]:

$$
\begin{bmatrix} u_{sx} \\ u_{sy} \\ u_{rx} \\ u_{ry} \end{bmatrix} = \begin{bmatrix} R_s & 0 & 0 & 0 \\ 0 & R_s & 0 & 0 \\ 0 & \omega_r L_m & R_r & \omega_r L_r \\ \omega_r L_m & 0 & \omega_r L_r & R_r \end{bmatrix}
\begin{bmatrix} i_{sx} \\ i_{sy} \\ i_{rx} \\ i_{ry} \end{bmatrix}
$$

$$
+ \begin{bmatrix} L_s & 0 & 0 & 0 \\ 0 & L_s & 0 & L_m \\ L_m & 0 & L_r & 0 \\ 0 & L_m & 0 & L_r \end{bmatrix} \frac{d}{dt}
\begin{bmatrix} i_{sx} \\ i_{sy} \\ i_{rx} \\ i_{ry} \end{bmatrix}.
$$

Also upon setting $\omega_g = \omega_s$ we get a matrix model of induction motor with respect to the reference frame rotating at a synchronous speed. Solving for the derivative of the current vector yields

$$
\begin{bmatrix} \dot{i}_{sx} \\ \dot{i}_{sy} \\ \dot{i}_{rx} \\ \dot{i}_{ry} \end{bmatrix} = \frac{1}{\Delta} \begin{bmatrix} R_s L_r & -\omega_r L_m^2 & -R_r L_m & -\omega_r L_m L_r \\ \omega_r L_m^s & R_s L_r & \omega_r L_m L_r & -R_r L_m \\ -R_s L_m & \omega_r L_m L_r & R_r L_s & \omega_r L_r L_s \\ \omega_r L_m L_s & -R_s L_m & -\omega_r L_r L_s & R_r L_s \end{bmatrix} \begin{bmatrix} i_{sx} \\ i_{sy} \\ i_{rx} \\ i_{ry} \end{bmatrix}
$$
$$
+ \begin{bmatrix} -L_r & 0 \\ 0 & -L_r \\ L_m & 0 \\ 0 & L_m \end{bmatrix} \begin{bmatrix} u_{sx} \\ u_{sy} \end{bmatrix} \tag{2.49}
$$

where $\Delta = L_m^2 - L_r L_s$. The output is given by

$$
\begin{bmatrix} i_{sx} \\ i_{sy} \end{bmatrix} = \begin{bmatrix} 1 & 0 & 0 & 0 \\ 0 & 1 & 0 & 0 \end{bmatrix} \begin{bmatrix} i_{sx} \\ i_{sy} \\ i_{rx} \\ i_{ry} \end{bmatrix} .
$$

Hence from above we obtain the following state space equation

$$
\dot{x} = Ax + Bu, \quad y = Cx + Du \tag{2.50}
$$

where $x = \begin{bmatrix} i_{sx} & i_{sy} & i_{rx} & i_{ry} \end{bmatrix}'$ is the state vector, and

$$A = \begin{bmatrix} R_s L_r & -\omega_r L_m^2 & -R_r L_m & -\omega_r L_m L_r \\ \omega_r L_m^s & R_s L_r & \omega_r L_m L_r & -R_r L_m \\ -R_s L_m & \omega_r L_m L_r & R_r L_s & \omega_r L_r L_s \\ \omega_r L_m L_s & -R_s L_m & -\omega_r L_r L_s & R_r L_s \end{bmatrix}$$

$$B = \begin{bmatrix} -L_r & 0 \\ 0 & -L_r \\ L_m & 0 \\ 0 & L_m \end{bmatrix}, \quad C = \begin{bmatrix} 1 & 0 & 0 & 0 \\ 0 & 1 & 0 & 0 \end{bmatrix}$$

and $D = \begin{bmatrix} 0 & 0 \\ 0 & 0 \end{bmatrix}$ are the realization matrices. The voltage vector $u = \begin{bmatrix} u_{sx} & u_{sy} \end{bmatrix}$ is the control input. Finally we state the expression for electromagnetic torque without derivation as:

$$T_e = 1.5P \frac{L_m}{L_r} (\psi_{rx} i_{sy} - \psi_{ry} i_{sx}) \tag{2.51}$$

where P the number of pole pairs of Induction motor. For more details please refer [16].

CHAPTER 3

FEEDBACK SYSTEM DESIGN

3.1 SISO Feedback Control System

Consider the discretized linear single-input/single-output (SISO) plant model $P(z)$ under the sampling frequency ω_s. Its input and output dynamics are conventionally represented by the nth order transfer function:

$$P(z) = \frac{b(z)}{a(z)} = \frac{b_m z^m + b_{m-1} z^{m-1} + ... + b_1 z + b_0}{z^n + a_{n-1} z^{n-1} + ... + a_1 z + a_0}. \tag{3.1}$$

Assume that $a(z)$ and $b(z)$ are coprime. Then $a(z)$ is the characteristic equation of the system, and its roots are poles of the system and determine stability of the system. It is well known that if the roots of characteristic equation lie strictly within the unit circle, the system is stable. However for design of feedback control system, stability alone is not adequate. Performance requirements in time domain and frequency domain are often imposed.

Consider the feedback control system in Figure 3.1. The closed-loop system admits transfer function

$$T(z) = \frac{K(z)P(z)}{1 + K(z)P(z)}. \tag{3.2}$$

The task for the designer is to synthesize $K(z)$ so that the performance requirements are
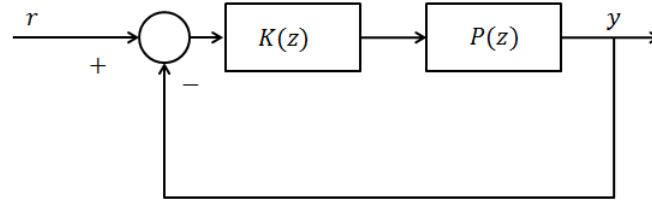
Figure 3.1

Negative Feedback

met.

In general there are two ways for design of the feedback control system. One is the time domain approach in which performance is specified by reference tracking, and noise/disturbance rejection etc. According to [9], time domain specifications include maximum overshoot, rise time, delay time, settling time, damping ratio, damping factor, natural undamped frequency, and steady state error. The graphical root locus provides a design tool in time domain which is aimed to assign the closed-loop poles into the desired locations and to ensure the design specifications in time domain. The second method widely used for design of the feedback control system is based on frequency response, i.e., the frequency domain method. The major design procedures in frequency domain includes the Nyquist criterion, the Bode plot, and the Nichols chart. Among them the Bode plot is more powerful in synthesizing the feedback controller, and it can be extended to MIMO systems as well. For this reason, a detailed explanation for Bode plot is provided.

Frequency response of the system is the steady state response to a sinusoidal input signal with sweeping frequencies. Bode diagram consists of a magnitude plot $|PK(e^{j\omega})|$ and phase angle plot $\angle PK(e^{j\omega})$ of the open loop system over a range of frequencies. The bandwidth of the magnitude response determines how fast the system responds to the input signal in time domain. High gain in low frequency range and small gain in high frequency gain determine the tracking and noise rejection. More important concepts are gain and phase margins.

Consider the feedback system as shown in Figure 3.1. The gain margin is defined as:

$$\text{GM} = 20\log_{10}\frac{1}{|PK(e^{j\omega_p})|}dB \tag{3.3}$$

where $|PK(e^{j\omega_p})|$ is the magnitude of $PK(e^{j\omega})$ measured at the frequency point ω_p, which is the frequency at which the phase of $P(e^{j\omega})$ is 180 degrees and which is called phase crossover frequency. The GM represents the maximum gain variation the feedback system can tolerate before it goes into instability. However gain margin alone is not adequate. A feedback system with good gain margin can have small stability margin, because of the variation of the phase of the transfer function. Hence phase margin is also indispensable. To find phase margin, the magnitude crossover frequency ω_c at which $|PK(e^{j\omega_c})| = 1$ needs to be located first. The phase margin is defined as:

$$\text{PM} = \left|\angle PK(e^{j\omega_c}) \pm 360°\right|. \tag{3.4}$$

3.2 MIMO Design Problem and Specifications

Many design methods are now available for MIMO (multi input multi output) feedback control systems. These methods include pole-placement, H-infinity robust control, optimal or LQR control, H-infinity loop shaping and LQR control with loop shaping. The design method to be considered in this thesis is LQR control based on loop shaping and LTR, with induction motor control as the application platform.

For a MIMO system with m-input and p-output, its transfer matrix has the form

$$P(z) = \begin{bmatrix} P_{11}(z) & \cdots & P_{12}(z) \\ \vdots & \cdots & \vdots \\ P_{p1}(z) & \cdots & P_{pm}(z) \end{bmatrix} \tag{3.5}$$

where $P_{ij}(z)$ represents the transfer function between jth input and ith output. Consequently the methods used for SISO analysis and controller design will either have to be modified or abandoned. The graphical root locus is difficult to be extend to MIMO systems. However there is a possibility to extend the Bode magnitude plot to MIMO systems. Such an extension is represented by the loop shaping method.

As observed in the SISO case the design specifications in frequency domain are mainly the gain margin and bandwidth of the magnitude plot, and phase margin of the phase plot. The main issue in the multivariable feedback design as stated in [11] is that a matrix does not have a unique gain, the norm $\|P(z)u(z)\|$ depends on the direction of the vector $u(z)$. Hence the induced norm is employed that is the maximum singular value at each frequency:

$$\|P(e^{j\omega})\| := \overline{\sigma}[P(e^{j\omega})] = \sup \frac{\|P(e^{j\omega})U(e^{j\omega})\|}{\|U(e^{j\omega})\|}. \tag{3.6}$$

It is well known that $\overline{\sigma}^2(A)$ is the maximum eigenvalue of A^*A or AA^*. In many cases, not only the maximum singular value, but also other singular values may also be used. Hence the plot of the singular values of the frequency response of the system for MIMO systems acts as the magnitude plot. The design specifications are often given in terms of the singular value plots of the system.

Consider a feedback system as shown in Figure 3.2. Difference from Figure 3.1, the input and output signals in Figure 3.2 are vector-valued. The vector signals in Figure 3.2 are clarified as next:

- r is the reference input.

- η measurement noise.

- d_i disturbance at plant input.

- d disturbance at plant output.

For simplicity, it is assumed that the disturbances d_i and d are white noises. The plant model $P(z)$ is a mathematical description of the relationship between the plant input and output.

MIMO systems are different from the SISO ones. Specifically the loop transfer matrix and sensitivity are not unique. The following are the basic terminologies used to specify the performance requirements for a standard feedback design as stated in [3] and [20]. The central idea for controller design using loop shaping as stated in [4] is formed around the
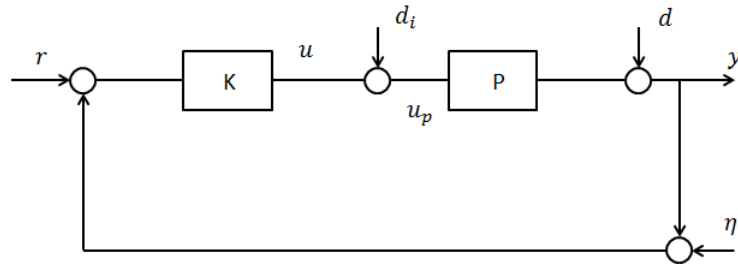
Figure 3.2

Standard Feedback System [20] (p-81)

fact that, the magnitude of the singular values of the closed loop system can be obtained using the corresponding open loop singular values.

- Input loop transfer matrix $L_i = KP$ is obtained by breaking the loop at the input u of the plant .

- Output loop transfer matrix $L_o = PK$ is obtained by breaking the loop at the output y of the plant.

- Input sensitivity matrix $S_i = (I + L_i)^{-1}$ is the transfer function between u_p and d_i as shown in Figure 3.2.

- Output sensitivity matrix $S_o = (I + L_o)^{-1}$ is the transfer function between y and d as shown in Figure 3.2.

- Input complementary sensitivity matrix is $T_i = I - S_i = L_i(I + L_i)^{-1}$.

- output complementary sensitivity matrix is $T_o = I - S_o = L_o(I + L_o)^{-1}$

33

By assuming that the system is internally stable, the following equations hold [20](page-82):

$$y = T_o(r - \eta) + S_o P d_i + S_o d, \tag{3.7}$$

$$r - y = S_o(r - d) + T_o \eta - S_o P d_i, \tag{3.8}$$

$$u = K S_o(r - \eta) - K S_o d - T_i d_i, \tag{3.9}$$

$$u_p = K S_o(r - \eta) - K S_o d + S_i d_i. \tag{3.10}$$

The above equations help to explain the relations between the design objectives and the transfer functions of the feedback system. From (3.8), the effects of disturbance d on the output of the system is suppressed, if S_o output sensitivity transfer matrix is made small which also reduces the effects of disturbance d. "By making transfer function small we mean to make the magnitude of frequency response singular values small, i.e. $\overline{\sigma}[S_o(e^{j\omega})] <<$ 1 over the operating frequency range."[20] (page-82) Similarly from (3.10), effects of disturbance d_i can be minimized if S_i is minimized. It means that the effects of disturbance d to the plant output are effectively desensitized.

More specifically from (3.8) and (3.10), in order to obtain good disturbance rejection at the plant output, the following singular values need to be made small at low frequencies:

$$\overline{\sigma}(S_o) = \overline{\sigma}(I + PK)^{-1} = \frac{1}{\underline{\sigma}(I + PK)},$$

$$\overline{\sigma}(S_o P) = \overline{\sigma}((I + PK)^{-1} P) = \overline{\sigma}(P S_i). \tag{3.11}$$

And in order to have disturbance rejection at the plant input following transfer functions should be made small at lower frequencies:

$$\overline{\sigma}(S_i) = \overline{\sigma}((I + KP)^{-1}) = \frac{1}{\underline{\sigma}(I + KP)},$$

$$\overline{\sigma}(S_i K) = \overline{\sigma}(K(I + PK)^{-1}) = \overline{\sigma}(KS_o). \tag{3.12}$$

As observed the above input sensitivity and output sensitivity have different expressions when $P(z)$ is of the size $p \times m$. For the case $p < m$, the rank $\{K(z)P(z)\} < p \ \forall |z| = 1$. Thus $\overline{\sigma}[S_i(e^{j\omega})]$ cannot be made smaller than 1. In this case, sensitivity minimization has to be carried out at the output of the plant. Similarly for the case $p > m$, rank $\{P(z)K(z)\} < m \ \forall |z| = 1$. Consequently $\overline{\sigma}[S_o(e^{j\omega})]$ cannot be made smaller than 1. Hence sensitivity minimization for this case has to be carried out at the plant input. See [6] for more detail.

3.3 Linear Quadratic Regulator

For MIMO systems, LQR continues to be a powerful synthesis tool. This section provides a brief description of the problem and solution.

Problem statement: Consider a discrete time system described by

$$x(k + 1) = Ax(k) + Bu(k), \quad x(0) = x_0 \neq 0 \tag{3.13}$$

where $u(k)$ of dimension m is the control input, and $x(k)$ of dimension n is the state. The objective is to minimize the quadratic cost

$$J = \sum_{k=0}^{\infty} x(k)' Q_f x(k) + u(k)' R u(k). \tag{3.14}$$

The weighting matrix $Q_f \geq 0$ represents the penalty on the state vector, and $R > 0$ represents the penalty on the control input.

Solution: Suppose that (A, B) is stabilizable and (Q_f, A) does not have unobservable modes on the unit circle. Then the solution to the above problem is the state feedback law $u(t) = Fx(t)$ specified by

$$F = -(R + B^* X B)^{-1} B^* X A, \tag{3.15}$$

$$X = A^* X A + Q_f - A^* X B (R + B^* X B)^{-1} B^* X A. \tag{3.16}$$

The above solution assumes that the system's states are available for feedback. If this is not the case, then output feedback control has to be used that results in the standard LQG control based on the separation principle [11]. In LQG control, the optimal estimate of the system state is used in feedback control. It assumes that

$$x(k+1) = Ax(k) + Bu(k) + B_1 d(k), \quad y(k) = Cx(k) + Dd(k)$$

where $d(t)$ is wide-sense stationary process with mean zero and covariance I. Assumes that (C, A) is detectable and (A, B_1) does not have unreachable modes on the unit circle. Then the optimal state estimator is given by

$$\widehat{x}(k+1) = A\widehat{x}(k) + Bu(k) - L[y(k) - \widehat{y}(k)], \tag{3.17}$$

$$= (A + LC)\widehat{x}(k) + Bu(k) - Ly(k). \tag{3.18}$$

where $\widehat{y}(t) = C\widehat{x}(k)$. The optimal state estimator gain L is obtained from

$$L = -AYC^*(DD^* + CYC^*)^{-1}, \tag{3.19}$$

$$Y = AYA^* + B_1B_1^* - AYC^*(DD^* + CYC^*)^{-1}CYA^*. $$

Combining the state feedback $u(k) = F\widehat{x}(k)$ and the estimator leads to

$$x(k+1) = Ax(k) + BF\widehat{x}(k) + B_1d(k), \tag{3.20}$$

$$\widehat{x}(k+1) = (A + BF + LC)\widehat{x}(k) - LCx(k) - LDd(k). \tag{3.21}$$

Let $e(k) = x(k) - \widehat{x}(k)$ be the state estimation error. Then taking the difference between the above two equations yields

$$e(k+1) = (A + LC)e(k) + (B_1 + LD)d(k). \tag{3.22}$$

Combining the above with $x(k+1) = Ax(k) + BF\widehat{x}(k) + B_1d(k)$ leads to

$$\begin{bmatrix} x(k+1) \\ e(k+1) \end{bmatrix} = \begin{bmatrix} A + BF & BF \\ 0 & A + LC \end{bmatrix} \begin{bmatrix} x(k) \\ e(k) \end{bmatrix} + \begin{bmatrix} B \\ B_1 + LD \end{bmatrix} d(k). \tag{3.23}$$

As a result, the closed loop eigenvalues are those eigenvalues of the optimal state feedback plus those of the optimal state estimation. The separation principle states that optimal state feedback and optimal state estimation result in an optimal solution to LQG control.

3.4 Loop Shaping Based on LQR

The optimal state feedback and state estimation can be used to shape the frequency response of the loop transfer matrix. The Lemma below is useful and concerns with the fact that sensitivity and complementary sensitivity transfer matrices constitute the coprime factors of the plant if F and L are stabilizing. Specifically the right coprime factorization corresponds to the state feedback/LQR and left coprime factorization corresponds to the Kalman filter/observer

Lemma 1. *[6] Consider the plant model $P(z) = C(zI - A)^{-1}B$ where (A, B) is stabilizable and (C, A) is detectable.*

(i) If $F = -(I + B'XB)^{-1}B'XA$ with $X \geq 0$ is the stabilizing solution to

$$X = A'XA - A'XB(I + B'XB)^{-1}B'XA + C'C, \tag{3.24}$$

then for all $|z| = 1$ there holds the identity

$$S_F(z)^* S_F(z) + S_F(z)^* T_F(z) = I + B'XB. \tag{3.25}$$

Furthermore, let $\Omega_F^* \Omega_F = I + B'XB$, then

$$\{\tilde{M}(z), \tilde{N}(z)\} = \{S_F(z)\Omega_F^{-1}, T_F(z)\Omega_F^{-1}\} \tag{3.26}$$

constitutes the pair of normalized right coprime factors of $P(z)$.

38

(ii) If $L = -AYC'(I + CYC')^{-1}$ with $Y \geq 0$ is the stabilizing solution to

$$Y = AYA' - AYC'(I + CYC')^{-1}CYA' + BB', \qquad (3.27)$$

then for all $|z| = 1$ there holds the identity

$$S_L(z)S_L(z)^* + T_L(z)T_L(z)^* = I + CYC'. \qquad (3.28)$$

Let $\Omega_L \Omega_L^* = I + CYC'$. Then

$$\{M(z), N(z)\} = \{\Omega_L^{-1} S_L(z), \Omega_L^{-1} T_L(z)\} \qquad (3.29)$$

constitutes the pair of normalized left coprime factors of $P(z)$.

It is noted that the following normalization properties

$$M(z)M(z)^* + N(z)N(z)^* = I,$$

$$\tilde{M}(z)^* \tilde{M} + \tilde{N}(z)^* \tilde{N} = I.$$

hold. Hence if the plant has the desired frequency shape, i.e., $\underline{\sigma}[P(e^{j\omega})]$ is large in the operating frequency range and $\overline{\sigma}[P(e^{j\omega})]$ is small in the high frequency range, then

$$\tilde{M}(e^{j\omega})\tilde{M}(e^{j\omega})^* = \left[I + P(e^{j\omega})^* P(e^{j\omega})\right]^{-1}, \qquad (3.30)$$

$$M(e^{j\omega})^* M(e^{j\omega}) = \left[I + P(e^{j\omega})P(e^{j\omega})^*\right]^{-1} \qquad (3.31)$$

resembles the ideal sensitivity at the plant input and output, respectively. Hence it can be concluded that if $\sigma_i\left[P(e^{j\omega})\right]$ admits the same shape as that of the desired loop transfer matrix, then for each integer i,

$$\sigma_i[\tilde{M}(e^{j\omega})] = \sigma_i[S_F(e^{j\omega})\Omega_F^{-1}] \tag{3.32}$$

represents the ideal sensitivity shape at the plant input and

$$\sigma_i[M(e^{j\omega})] = \sigma_i[\Omega_L^{-1}S_L(e^{j\omega})] \tag{3.33}$$

represents the ideal sensitivity shape at the plant output. In addition, by the normalization property,

$$\tilde{N}(e^{j\omega})\tilde{N}(e^{j\omega})^* = P(e^{j\omega})\left[I + P(e^{j\omega})^*P(e^{j\omega})\right]^{-1}P(e^{j\omega})^*, \tag{3.34}$$

$$N(e^{j\omega})^*N(e^{j\omega}) = P(e^{j\omega})^*\left[I + P(e^{j\omega})P(e^{j\omega})^*\right]^{-1}P(e^{j\omega}). \tag{3.35}$$

Hence if $\sigma_i\left[P(e^{j\omega})\right]$ admits the same shape as that of the desired loop transfer matrix for each integer i,

$$\sigma_i[\tilde{N}(e^{j\omega})] = \sigma_i[T_F(e^{j\omega})\Omega_F^{-1}] \tag{3.36}$$

represents the ideal complementary sensitivity shape at the plant input and

$$\sigma_i[N(e^{j\omega})] = \sigma_i[\Omega_L^{-1}T_L(e^{j\omega})] \tag{3.37}$$

represents the ideal complementary sensitivity shape at the plant output. Consequently, if the shape of $P(z)$ is designed to achieve the desired loop shape, the state feedback gain F achieves the desired input sensitivity, and the state estimation gain L achieves the desired output sensitivity.

In the case when the open loop plant does not admit the desired frequency shape, the procedure outlined in [4] can be employed.

- The frequency response of a MIMO system can be shaped by pre and post multiplication of some weighting $W_1(z)$ and $W_2(z)$, respectively to compensate the loop shape.

- A feedback controller $K_w(z)$ is then designed for the weighted plant
$P_W(z) = W_2(z)P(z)W_1(z)$.

- The feedback controller and the compensator/weighting function are combined to form a final controller $K(z) = W_1(z)K_w(z)W_2(z)$.

Figure 3.3 below shows the implementation of loop shaping method.
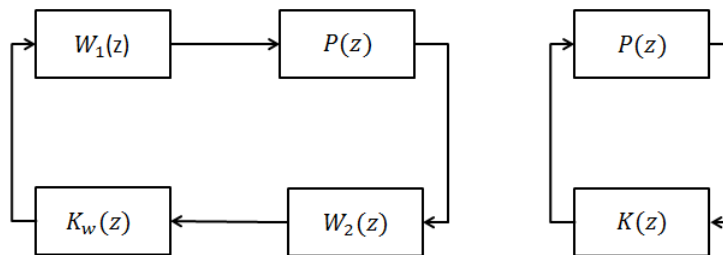
Figure 3.3

Illustration of Loop Shaping Procedure-[4](p-107)

3.5 Loop Transfer Recovery

For simplicity, we consider only the case of $p \geq m$. That is, the plant is tall or square. Hence the LTR procedure is employed to achieve the desired loop shape or desired sensitivity under state feedback. However the feedback compensator under output feedback may not be able to recover the the desired loop shape. An LTR procedure has been proposed in the literature [10],[11] which will be studied in this section.

There are two cases to consider. The first one assumes that the plant $P(z) = C(zI - A)^{-1}B$ is strictly minimum phase, has been squared down by weighting functions, and $\det(CB) \neq 0$. It is well known that perfect LTR can be achieved in the sense that a stabilizing output feedback controller $K(z)$ can be designed such that

$$K(z)P(z) = F(zI - A)^{-1}B \tag{3.38}$$

of which F is the optimal state feedback gain that achieves the desired loop shape.

Definition 1. *The transmission zeros of a system are defined as the set of complex numbers z_0 that satisfy the following inequality.*

$$rank \begin{bmatrix} z_0 I - A & B \\ -C & 0 \end{bmatrix} < n + m \tag{3.39}$$

Definition 2. *The system is said to be non-minimum phase, if at least one of its transmission zeros is outside the closed unit circle and such zeros are called non minimum phase zeros of the system.*

"The LTR procedure under strictly minimum phase and $\det(CB) \neq 0$ synthesizes the state estimation gain by solving the stabilizing solution $Y \geq 0$ to the following ARE:

$$Y = AYA^* - AYC^*(q^{-2}I + CYC^*)^{-1}CYA^* + BB^*. \tag{3.40}$$

The above ARE can be rewritten as

$$\bar{Y} = A\bar{Y}(I + CC^*\bar{Y})^{-1} + q^2BB^*$$

by taking $\bar{Y} = q^2Y$. If $q \to \infty$ in (3.40), then

$$Y = AYA^* - AYC^*(CYC^*)^{-1}CYA^* + BB^*.$$

Since $\det(CB) \neq 0, Y = BB^*$ satisfies the above equation. Hence the estimation gain becomes

$$L = -AYC^*(CYC^*)^{-1} = -AB(CB)^{-1}.$$

This corresponds to the case of perfect LTR [10]. We will prove this fact next.

Note first that

$$A + LC = A - AB(CB)^{-1}C = A[I_n - B(CB)^{-1}C]. \tag{3.41}$$

Since $\det(CB) \neq 0$, the plant model $P(z) = C(zI - A)^{-1}B$ has exactly $(n-m)$ zeros that are all inside the unit circle by the strictly minimum phase assumption. Direct calculation shows

$$
\begin{aligned}
zC(zI - A)^{-1}B &= CB + C(zI - A)^{-1}AB \\
&= [I + C(zI - A)^{-1}AB(CB)^{-1}]CB \qquad (3.42) \\
&= [I - C(zI - A)^{-1}L]CB.
\end{aligned}
$$

Taking inverse of the above square transfer matrix yields

$$
z^{-1}(C(zI - A)^{-1}B)^{-1} = (CB)^{-1}[I + C(zI - A - LC)^{-1}L].
$$

It follows that $(A + LC)$ is a stability matrix. Hence $Y = BB^*$ is the stabilizing solution to the filtering ARE (3.40) in the limiting case of $q \to \infty$.

The output feedback controller is taken as

$$
K(z) = -zF_1(zI - A - LC)^{-1}L, \quad F_1 = -(I + B^*XB)^{-1}B^*X \qquad (3.43)
$$

where $X \geq 0$ is the stabilizing solution to the ARE," [6]

$$
X = A^*X(I + BB^*X)^{-1}A + C^*C. \qquad (3.44)
$$

Recall that this is the same ARE for right normalized coprime factorization. As shown in [10], perfect LTR can be achieved.

44

Theorem 1. *[10] Consider the square plant model $P(z) = C(zI-A)^{-1}B$. If (i) $\det(CB) \neq 0$ and (ii)the realization of $P(z)$ is strictly minimum phase, then the equality $K(z)P(z) = F_1 A(zI - A)^{-1}B$ holds where $K(z)$ is the output feedback controller in (3.43).*

For completeness, we provide a proof here based on [10].

Proof. It is easy to observe that $\det(CB) \neq 0$ iff $R^n = range(B) \bigoplus \ker(C)$. Then $\Pi = B(CB)^{-1}C$ is a projector onto $range(B)$ along $\ker(C)$, and there hold $LC = -A\Pi$ and $(I - \Pi)B = 0$. Let

$$\delta(z) = F_1 A(zI - A)^{-1}B - K(z)P(z).$$

The proof of achieving a perfect recovery relies on proving $\delta(z) \equiv 0$:

$$\delta(z) = F_1 A(zI - A)^{-1}B + zF_1(zI - A - LC)^{-1}LC(zI - A)^{-1}B \qquad (3.45)$$

$$= F_1 A(zI - A)^{-1}B - zF_1(zI - A + A\Pi)^{-1}A\Pi(zI - A)^{-1}B \qquad (3.46)$$

$$= F_1 A(zI - A)^{-1}B - zF_1 A[zI - (I - \Pi)A]^{-1}\Pi(zI - A)^{-1}B \qquad (3.47)$$

$$= F_1 A(zI - (I - \Pi)A)^{-1}[zI - (I - \Pi)A - z\Pi](zI - A)^{-1}B \qquad (3.48)$$

$$= F_1 A[zI - (I - \Pi)A]^{-1}[(I - \Pi)(zI - A)](zI - A)^{-1}B \equiv 0 \qquad (3.49)$$

as $(I - \Pi)B = 0$. $\qquad\qquad\qquad\qquad\qquad\qquad\qquad\qquad\qquad\qquad\qquad\qquad \square$

In conclusion the perfect recovery is achieved. Intuitively, $K(z)$ has m poles at the origin which are cancelled by m zeros at the origin due to z in the front. The remaining $(n - m)$ poles of $K(z)$ are cancelled by the $(n - m)$ finite zeros of $P(z)$ which are all

stable by the strictly minimum phase assumption. It needs to be pointed out that the perfect LTR fails, if the plant is non-minimum phase plant, and/or $\det(CB) = 0$. Hence a different design procedure needs to be developed for non-minimum phase plants. The following is a result that helps to factorize the non-minimum phase zeros of the plant [6].

Lemma 2. *[6] Consider the square plant model $P(z) = C(zI - A)^{-1}B$ with stabilizable and detectable realization. If $P(z)$ has full normal rank void zeros on the unit circle, then the following factorization holds:*

$$P(z) = C_a(z)P_m(z), \quad P_m(z) = C_m(zI - A)^{-1}B, \tag{3.50}$$

where $C_a(z)$ is a square inner (all pass and stable), the realization of $P_m(z)$ is strictly minimum phase, and $\det(C_m B) \neq 0$.

Proof. By hypothesis, there exists an integer $\kappa \geq 0$ such that $CA^\kappa B \neq 0$. If $\kappa > 0$, then $CA^i B = 0$ for $0 \leq i < \kappa$. Denote $D_\kappa = CA^\kappa B$ and $C_\kappa = CA^{\kappa+1}$. Then

$$z^{\kappa+1}P(z) = P_i(z)P_o(z).$$

From spectral factorization theory, if A is a stability matrix then

$$z^{\kappa+1}P(z) = P_i(z)P_o(z)$$

with $P_i(z)$ an inner and $P_o(z)$ an outer. If A is not a stability matrix, then $P_o(z)$ is strictly minimum phase. Specifically let $R_\kappa = D_\kappa^* D_\kappa$ and $Z \geq 0$ be the stabilizing solution to the ARE

$$Z = A^* Z A + C_\kappa^* C_\kappa - (A^* Z B + C_\kappa^* D_\kappa)(R_\kappa + B^* Z B)^{-1}(B^* Z A + D_\kappa^* C_\kappa).$$

The full normal rank condition on $P(z)$ implies that $\Omega^2 = R_\kappa + B^* Z B$ is nonsingular. The state feedback gain $F_\kappa = -(R_\kappa + B^* Z B)^{-1}(D_\kappa^* C_\kappa + B^* Z A)$ is stabilizing. Moreover $P_i(z)$ and $P_o(z)$ have the following expressions:

$$P_i(z) = \left[\begin{array}{c|c} A + BF_\kappa & B \\ \hline C_\kappa + D_\kappa F_\kappa & D_\kappa \end{array}\right] \Omega^{-1}, \quad P_o(z) = \Omega \left[\begin{array}{c|c} A & B \\ \hline -F_\kappa & I \end{array}\right].$$

Note that $F_\kappa = \widehat{F}_\kappa A$ where

$$\widehat{F}_\kappa = -(R_\kappa + B^* Z B)^{-1}(D_\kappa^* C A^\kappa + B^* Z).$$

Using the expressions of R_κ and D_κ yields

$$R_\kappa + B^* Z B = B^* (A^{*\kappa} C^* C A^\kappa + Z) B,$$

$$D_\kappa^* C A^\kappa + B^* Z = B^* (A^{*\kappa} C^* C A^\kappa + Z).$$

47

It follows that $I = -\widehat{F}_\kappa B$ and thus

$$P_o(z) = -\Omega \left[\begin{array}{c|c} A & B \\ \hline \widehat{F}_\kappa & \widehat{F}_\kappa B \end{array} \right] = -z\Omega\widehat{F}_\kappa \left(zI - A \right)^{-1} B.$$

By setting $C_a(z) = z^{-\kappa}P_i(z)$ and $C_m = -\Omega\widehat{F}_\kappa$ leads to the factorization in (3.50). Since $\det(C_m B) \neq 0$ and zeros of $P_o(z)$ are eigenvalues of $(A + BF_\kappa)$ which are all stable, $P_m(z) = C_m(zI - A)^{-1}B$ is indeed strictly minimum phase. The proof is complete. $\square$

The LTR procedure will be applied to $P_m(z)$ that is strictly minimum phase and satisfies $\det(C_m B) \neq 0$. Feedback controller remains the same except that L is replaced by

$$L_m = -AB(C_m B)^{-1}.$$

Clearly the perfect recovery is not possible. The following result from [19] shows how much the target loop can be recovered. The proof is omitted.

Theorem 2. *[10, 6] Suppose that $P(z)$ is factorized as in lemma 2 and the LTR applied to $P_m(z)$. Under the stabilizability and detectability condition,*

$$P(z)K(z) = [H(z) - E(z)] [I - E(z)]^{-1} \tag{3.51}$$

where $H(z) = F(zI-A)^{-1}B$ is the targeted loop transfer matrix and $E(z) = [C - C_a(z)C_m] (zI - A)^{-1}L$ is the error function.

48

For MIMO system the design approach is bifurcated into two major categories, i.e. the design procedure for the minimum phase plant and for the design procedure the non-minimum phase plant. We summarize the design procedure in following steps:[6]

Given a plant $P(z) = C(zI - A)^{-1}B$ where $p \geq m$, following are the steps followed for the controller design in case of the minimum phase plant:

- Carry out the frequency shaping for the plant by adding weighting function at the plant input. Name the weighted plant as $P_w(z)$.

- Design the state feedback using the ARE in (3.44) as $F = F_1A$, where $F_1 = -(I + B^*XB)^{-1}B^*X$.

- Design the Optimal estimator $L = -AB(CB)^{-1}$ for minimum phase plant.

- For the case where the plant is non-minimum phase, the state feedback F obtained as in minimum phase case. Compute factorization $P(z) = C_a(z)P_m(z)$ following Lemma 2, $C_a(z)$ is the square inner and $P_m(z) = C_m(zI - A)^{-1}B$ is strictly minimum phase.

- Design an estimator $L = -AB(C_mB)^{-1}$ using $P_m(z)$ from previous step, for perfect recovery of the factorized minimum phase plant.

Hence final controller is the combination of the estimator and the state feedback. For either of the case, set $L_0 = F_1L$ where F_1 is same as in (3.43) and noting that $F = F_1A$. Hence we obtain the following controller.

$$K(z) = \left[\begin{array}{c|c} A + BF + LC + BL_0C & L + BL_0 \\ \hline F + L_0C & L_0 \end{array} \right].$$

CHAPTER 4

SIMULATION AND RESULTS

4.1 Controller Design and Matlab Simulation

For experimental purpose we have chosen a $\frac{1}{2}$H.P industrial grade 3-phase induction motor. In order to implement the LQG/LTR controller on the induction motor the first step is to ascertain the motor parameters like R_s, R_r, L_s, L_r and L_m. By performing short circuit and noload test on the induction motor its parameters are determined as mentioned in table figure 4.1 The motor model is linearised at a fixed operating speed of ω_r=364 rad/sec.The

Motor Tests		
No Load Test		
Frequency	60	Hz
Voltage(L-L)	226	V
Current(Line)	1.36	A
Input Power	180	Watts
Short Circuit test		
Frequency	60	Hz
Voltage (L-L)	46.93	V
Current(Line)	2.02	A
Input Power	141	Watts
Motor Parameters		
Stator	Rotor	
R_s=5.83	R_r=5.6885	Ω
$L_s = L_{ls} + L_m = 0.2532$	$L_r = L_{lr} + L_m = 0.2569$	Henry

Figure 4.1

Motor Tests

stator and rotor current components form the state variables specified by

$$x(t) = \begin{bmatrix} i_{sd} & i_{sq} & i_{rd} & i_{rq} \end{bmatrix}^T.$$

The stator voltages and currents

$$u(t) = \begin{bmatrix} V_{sd} \\ V_{sq} \end{bmatrix}, \quad y(t) = \begin{bmatrix} i_{sd} \\ i_{sq} \end{bmatrix}$$

are the control inputs and output of the system, respectively. The state space description of

the actual system is given by

$$\dot{x}(t) = Ax(t) + Bu(t), \tag{4.1}$$

$$y(t) = Cx(t) \tag{4.2}$$

where

$$A = \begin{bmatrix} -328.6851 & 4832.1 & 307.0950 & 5046.3 \\ -4832.1 & -328.6851 & -5046.3 & 307.0950 \\ 314.7339 & 5046.3 & -316.2116 & -5196.1 \\ 4975.5 & 314.7339 & 5196.1 & -316.2116 \end{bmatrix}, \tag{4.3}$$

$$B = \begin{bmatrix} 56.3782 & 0 \\ 0 & 56.3782 \\ -53.9852 & 0 \\ 0 & -53.9852 \end{bmatrix}, C = \begin{bmatrix} 1 & 0 & 0 & 0 \\ 0 & 1 & 0 & 0 \end{bmatrix}. \tag{4.4}$$

$$\tag{4.5}$$

We assume that the specification for the induction motor control is given in time domain. The design specs are maximum overshoot no more than 5 percent, and settling time no more than 0.05 seconds. For the given open loop frequency response of the linearised system, the weighting function is chosen so as to increase the bandwidth of the plant along, and the open loop gain at low frequencies. The use of weighting functions enhances the performance characteristics and better disturbance rejection. Starting with a simple PI compensator and after several iterations, we choose following weighting function at the plant input.

$$W = \frac{3.5s + 1225}{s} \tag{4.6}$$

The weighting function is selected such that the gain crossover frequency is close to 1000 rad/sec. Figure 4.2 is the open loop and the weighted plant frequency response of the system. The final controller $K(z) = \hat{D} + \hat{C}(zI - \hat{A})^{-1}\hat{B}$ is computed according to the LQG/LTR procedure studied in the previous chapter where
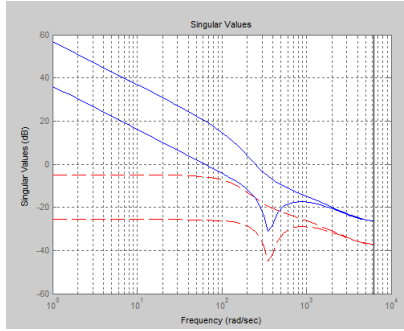
Figure 4.2

Open loop weighted and nominal plant frequency response

$$
\hat{A} = \begin{bmatrix}
0.9373 & 0.0218 & -0.3045 & 0.0071 & -0.1651 & 0.0072 \\
0.0413 & 0.8647 & 0.2911 & -0.3316 & 0.3189 & -0.2137 \\
0.5655 & 0.1267 & -0.6200 & 2.0408 & -0.6211 & 2.1702 \\
0.2399 & 0.1466 & -0.3056 & -0.8533 & -0.2880 & -0.9252 \\
-0.5427 & -0.1238 & 1.5212 & -2.0756 & 1.5704 & -2.2272 \\
-0.2285 & -0.1397 & 0.4572 & 1.7435 & 0.4530 & 1.8552
\end{bmatrix}
\tag{4.7}
$$

$$
\hat{B} = \begin{bmatrix}
-0.1396 & -0.0109 \\
-0.0212 & -0.0956 \\
-0.7197 & -0.1072 \\
-0.0603 & -0.5529 \\
0.6741 & 0.1517 \\
0.0516 & 0.5223
\end{bmatrix}
\tag{4.8}
$$

$$
\hat{C} = \begin{bmatrix}
-3.9176 & 1.3628 & -9.2322 & 0.0158 & -10.3199 & 0.4495 \\
2.5813 & -8.4553 & 18.6624 & -11.1063 & 19.9301 & -13.3583
\end{bmatrix}
\tag{4.9}
$$

53

$$\hat{D} = \begin{bmatrix} -1.0760 & 1.1072 \\ 0.8597 & -3.6461 \end{bmatrix} \qquad (4.10)$$

As discussed in the previous chapter, the controller admits left coprime factorization:

$$K(z) = V(z)^{-1}U(z) \qquad (4.11)$$

The two-degree-of-freedom controller employs $V(z)^{-1}\Omega_f^{-1}$ as the feed forward controller, and $K(z)$ as the feedback controller which is shown in the following figure 4.3
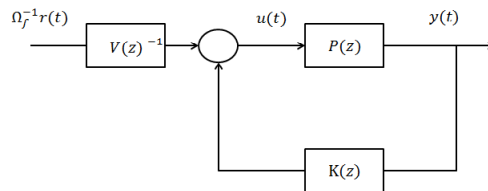
Figure 4.3

Two degree of freedom control system - [6]

4.2 Closed Loop Response Analysis

Figures 4.4 and 4.5 are the plots of closed loop singular values plot of the system transfer function and the sensitivity function plot and step response of the closed loop system. As it is evident that the closed loop sensitivity function has significantly smaller gain at lower frequency and for higher frequency it is close to 0 db.Such a frequency shape for

54

the sensitivity of the closed-loop system results in significantly reduced sensitivity to the disturbance. The step response has a settling time of 73.3 and 79.9 samples, and thus satisfying the design specs. Recall that the sampling frequency is 2000 Hz. The step response shows an approximately 0 percent steady state error, which is due to the integrator in weighting function. Percentage Overshoot is 4.38% and 0% for two outputs respectively.
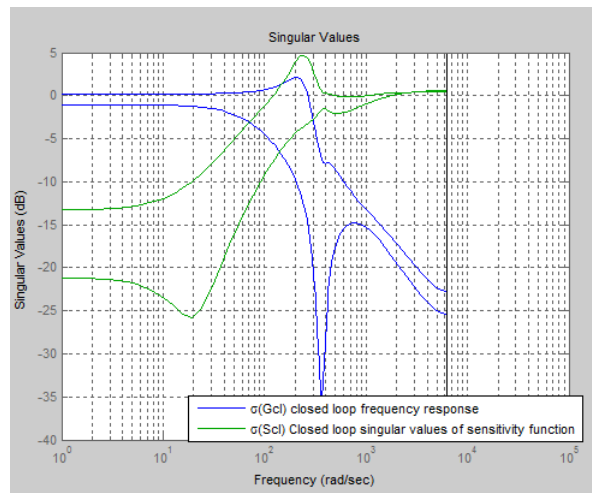
Figure 4.4

Singular values plot of the closed loop system and the Sensitivity function

4.3   Implementation of the Controller

After designing the final controller next task is to determine the implementation. The model used to solve the control problem incorporates the electrical dynamics of the system. Hence the design requirements chosen are such that they specify the related performances. Below mentioned figure explains and the ®Matlab ™Simulink diagram modified from the demo
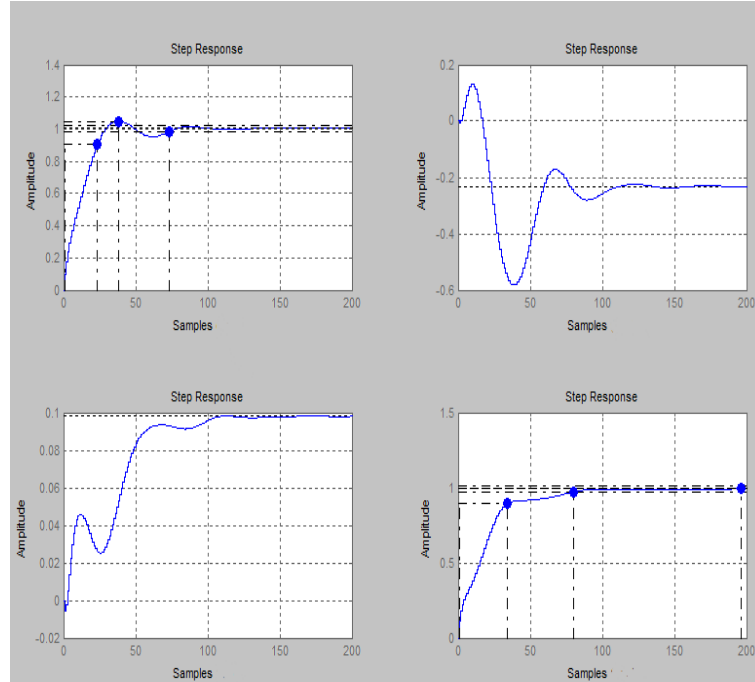
Figure 4.5

Step response of the Closed loop system

of ®SimPowerSystem toolbox. In figure 4.6, there are two actions a) speed control and b)current control. The speed control is a simple Proportional Integral controller which converts the speed error into the required electromagnetic torque. The electromagnetic torque and voltage equations in general frame of induction motor is reproduced from Chapter 2.

$$T_e = 1.5P\frac{L_m}{L_r}(\psi_{rx}i_{sy} - \psi_{ry}i_{sx})$$

$$u_{sy} = R_s i_{sy} + \frac{d}{dt}\psi_{sy} + \omega_g\psi_{sx}$$

$$u_{sx} = R_s i_{sx} + \frac{d}{dt}\psi_{sx} - \omega_g\psi_{sy} \tag{4.12}$$

$$0 = R_r i_{ry} + \frac{d}{dt}\psi_{ry} + (\omega_g - \omega_r)\psi_{rx} \tag{4.13}$$

$$0 = R_r i_{rx} + \frac{d}{dt}\psi_{rx} - (\omega_g - \omega_r)\psi_{ry} \tag{4.14}$$

where

$$\psi_{sy} = L_s i_{sy} + L_m i_{ry} \tag{4.15}$$

$$\psi_{sx} = L_s i_{ds} + L_m i_{rx} \tag{4.16}$$

$$\psi_{ry} = L_r i_{ry} + L_m i_{sy} \tag{4.17}$$

$$\psi_{rx} = L_r i_{rx} + L_m i_{sx} \tag{4.18}$$

"The indirect field-oriented control requires that the i_{sx} component of the stator current is aligned with the rotor field and the component i_{sy} is perpendicular to i_{sy}. This is achieved by choosing ω_g to be the speed of the rotor flux such that the rotor flux is aligned precisely with the d axis, resulting in

$$\psi_{ry} = 0 \Rightarrow \frac{d}{dt}\psi_{ry} = 0 \tag{4.19}$$

and $\psi_{rx} = |\bar{\psi}_{rg}|$ (a scalar quantity) which implies that difference

$$(\omega_g - \omega_r) = \frac{L_r R_r}{\psi_{rg} L_r} i_{sy} \tag{4.20}$$

using equations 4.13,4.17 , hence $T_e = 1.5 P \frac{L_m}{L_r}(\psi_{rg} i_{sy})$. Also using 4.20 and 4.14

$$\frac{d}{dt}\psi_r = -\left(\frac{R_r}{L_r}\right)\psi_r + \left(\frac{L_m R_r}{L_r}\right) i_{ds} \tag{4.21}$$

Which makes the analogy with DC machine performance clear. The electric torque is directly proportional to the i_{sy} stator current component and ψ_r and i_{sx} are related by a

first order transfer function as seen in 4.21. Now following set of equations are used in the simulink model to obtain the reference current values i^*_{sx} and i^*_{sy}.

$$i^*_{sy} = \frac{2}{3}\frac{2}{P}\frac{L_r}{L_m}\frac{T^*_e}{|\psi_{rgE}|} \tag{4.22}$$

where $|\psi_{rgE}|$ is the estimated flux, given as $|\psi_{rgE}| = \frac{L_m i_{sx}}{1 + \frac{L_r}{R_r}s}$. The stator direct axis current
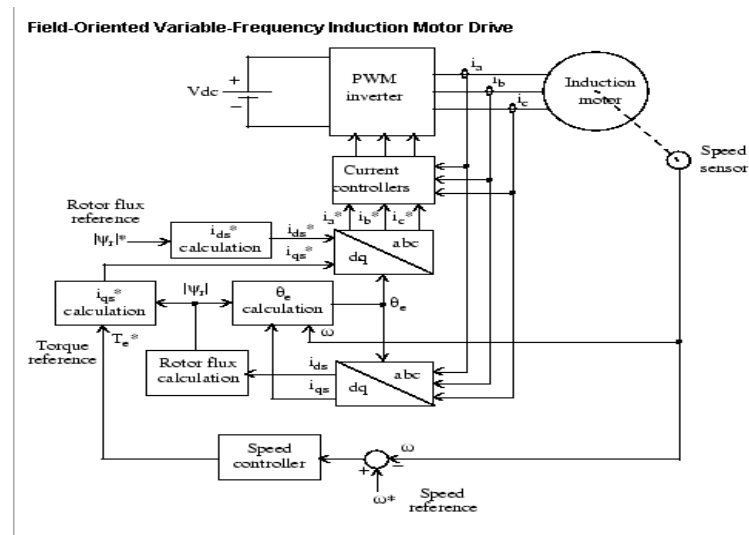
Figure 4.6

Field Oriented Control Block diagram - [13]

reference is $i^*_{sx} = \frac{|\psi_{rg}|^*}{L_m}$ where $|\psi_{rg}|^*$ is the reference/steady state calculated rotor flux value. Finally the rotor flux angle position is calculated as:"-[13]

$$\theta_e = \int (\omega_r + \frac{L_m R_r}{L_r |\psi_{rgE}|}i^*_{sy}) \tag{4.23}$$

Recall that the model developed in Chapter 2 was with $\omega_g = 0$, i.e. with respect to a stationary reference frame. In simulation we employ a abc-dq transformation with uses the calculated rotor flux angle position for the transformation.

The controller we designed $K(z)$ is used as the current controller in figure 4.6. The speed controller is $26 + \frac{13}{s}$ proportional controller. The final closed loop simulation is as shown in figure 4.9. The first plot is the step reference speed plot, second is the current applied to the motor third is the actual speed of the motor and the fourth plot is the torque generated by the motor.

4.4 Hardware Equipments

The hardware equipments used for the experimental purpose are as follows

- A ™TI DSP TMS320F2812 based evaluation board and 2812 High voltage Power Electronic Board.

- 3-phase $\frac{1}{2}$ Industrial grade class B induction motor.

- Current sensing hall effect sensor.

- 3 channel encoder.

- Spectrum digital JTAG emulator for programming and debugging the DSP.

The dsp used in the evaluation board is specifically designed for motor applications and has a 32 bit CPU with Harvard Bus Architecture. The Motor Control Peripherals on the dsp consists of two Event Managers (EVA, EVB) which support features like PWM units, capture units and quadrature encoder pulse circuits. Apart from this the DSP has an ADC

unit which is used to read the current data form the hall effect current sensor. The main features of the custom built EVM DSP along with power electronic board are:

- Configuration of 256K (Program 64K, data 64K) non-delay SRAM, clock frequency at 150MHz on board;

- 16-Channel 12 bit A/D internal converter;

- 128K Flash ROM is re-programmable;

- In-chip event organizer directly controls 12-channel PWM pulse outputs. 6 hardware acquisition units can connect to Hall signal and photoelectric encoder signal.

- In-chip SPI slot exchanges data with serial EEPROM for boot load function

- 250Kbps communications rate between RS232C interface and host

- On-board IEEE11.49.1JTAG slot supports system emulation and Flash ROM program

- On-board optical encoder input slot and Hall input slot

- AC 220V input, supplying power to control system

4.5 Software Implementation

For software implementation of the DSP, two major libraries provided by Texas Instruments are used extensively IQmath and DMC. IQmath library is a set of highly optimized and high precision mathematical functions which helps in implement seamlessly a floating-point algorithm into fixed point code on TMS320C28x devices. There are in all 30 data types which can be used for floating point operations, the resolution and max-min range

for these data types starts from 0.000000001 to 0.5 and -2 - 1.999999999, -1073741824-1073741823.500000000 respectively. The DMC library consists of list of functions which performs functions like data logging, park-clarke transformation, encoder reading, speed calculations, current measurements, space vector PWM generation etc.

The software implementation is done in two different modes, initialization mode and secondly run/Interrupt service subroutine mode. Following are the steps for ISR every time interrupt occurs:

- Speed and 2 out of 3 phase current measurements are carried out using QEP and SPEED_MEA library functions.

- Perform D-Q transformation and convert 3 phase current values to 2 phase.

- Estimate the stator flux and the rotor flux angle using the field Oriented Control equations.

- Calculate the speed error and using speed controller find the desired torque.

- Using reference flux and desired torque values find the i_{ds}^* and i_{dq}^* values.

- Apply the designed controller and using PWM generator calculate the pulse width required for the control input.

This concludes the calculation of controller, control scheme, simulation results and the basic information about the hardware and the software of DSP board.
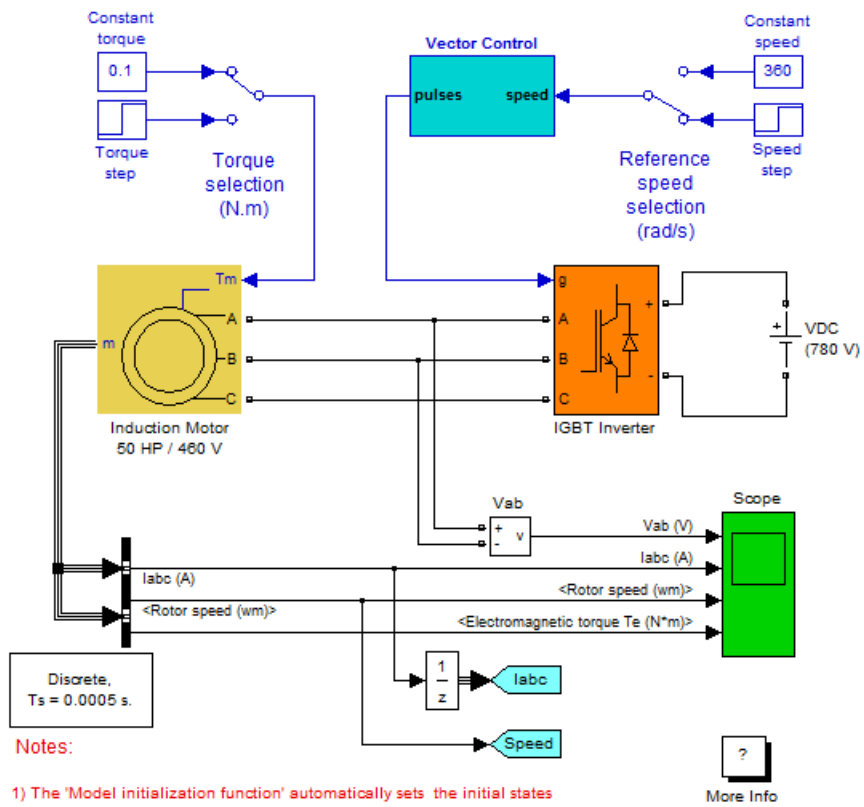
Figure 4.7

Simulink diagram for Vector Control in feedback mode-a [13]
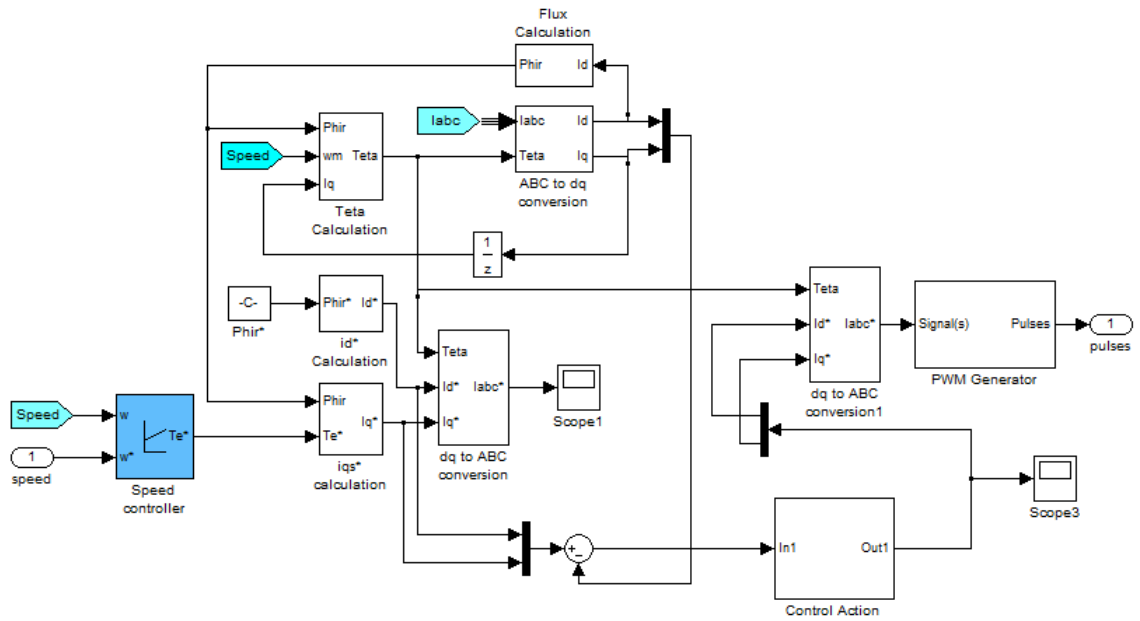
Figure 4.8

Simulink diagram for Vector Control in feedback mode-b [13]
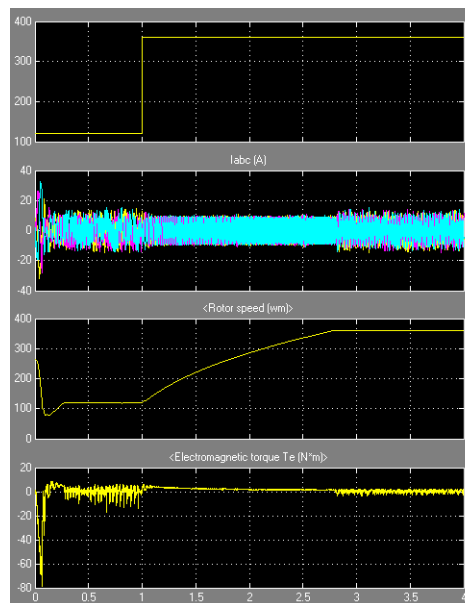
Figure 4.9

Simulation results

CHAPTER 5

CONCLUSIONS

The thesis addressed the problem of LQG/LTR design method for discrete time system using weighting functions. As observed from the simulation results we get a decent tracking of reference speed signal by the system, but there is a room for improvement as the responses are a bit sluggish. As encountered in the literature review, apart from the controller design, accurate estimation plays a major role in control of Induction motor. Since the plant is minimum phase, same procedure for controller design with a modified model, with rotor speed as state vector can be used. The benefit of doing so is that, sensor less vector control scheme can also be implemented. The progress of hardware implementation till now has been that a c/c++ based program for 3-phase fixed frequency supply generation through power electronic board has been accomplished. In order to implement the feedback control, a subroutine for current sensing and encoder reading is under development. Once these two subroutines are developed, the controller can be implemented and actual results can be obtained.

5.1 Future Scope of Study

Once the basic platform of test on Induction motor is developed, several other MIMO control methods can be tested with minor changes in the program. An obvious extension would be H-infinity control method and then compare the results of two methods. Discretised non-

linear controller can also form a challenging problem. In terms of theoretical development, an expression for stability margin in relation with the weighting function if developed can greatly smoothen the process of loop shaping and LQG design method. A generalization of LQG/LTR design method can also be extended to linear continuous-time systems. Since Induction motor is one of the most common control problem in Industrial domain the above mentioned problems can be of great interest.

REFERENCES

[1] Chen, Ben M., and Ya-Ling Chen. "Loop transfer recovery design via new observer based and ccs architecture-based controllers." International Journal of Robust and nonlinear control 5 (1995): 649-69.

[2] Ebrahim, O.S.; Salem, M.F.; Jain, P.K.; Badr, M.A.; , "Application of linear quadratic regulator theory to the stator field-oriented control of induction motors," *Electric Power Applications, IET* , vol.4, no.8, pp.637-646, Sept. 2010 doi: 10.1049/iet-epa.2009.0164

[3] J. C. Doyle, and G. Stein, "Multivariable feedback design: Concepts for a classical/-modern synthesis," *IEEE Trans. Automat. Contr.*, 26(1), pp. 4-16, 1981.

[4] Glover, Keith, and Duncan C. McFarlane. "A Loop Shaping Design Procedure." *Robust Controller Design Using Normalized Coprime Factor Plant Descriptions*. Berlin [etc.: Springer-Verlag, 1989. 98-106. Print.

[5] Green, Michael, and David J. N. Limebeer. *Linear Robust Control*. Englewood Cliffs, NJ: Prentice Hall, 1995. Print.

[6] Gu Guoxiang."Design of Feedback Control System." *Discrete-Time Linear Systems-Theory and Design with applications*. To be published by Springer, 2011.

[7] K. Young-Real, S. Seung-Ki, and P. Min-Ho, "Speed sensorless vector control of induction motor using extended Kalman filter," IEEE

[8] Krishnan, R. "Vector-Controlled Induction Motor Drives."*Electric Motor Drives: Modeling, Analysis, and Control.* Upper Saddle River, NJ: Prentice Hall, 2001. 411-14. Print.

[9] Kuo, Benjamin C., and Benjamin C. Kuo. *Digital Control Systems*. New York: Oxford UP, 1992. Print.

[10] Maciejowski, J. "Asymptotic Recovery for Discrete-time Systems." IEEE Transactions on Automatic Control 30.6 (1985): 602-05. Print.

[11] Maciejowski, Jan Marian. *Multivariable Feedback Design*. Wokingham, England: Addison-Wesley, 1989. Print.

[12] Marino, Riccardo, Patrizio Tomei, and Cristiano M. Verrelli. "Dynamical Models and Structural Properties." *Induction Motor Control Design*. London: Springer, 2010. 1-2. Print.

[13] ®Mathworks"Simulating an AC Motor Drive:Flux-oriented Control"mathworks.com.®Mathworks. 2011. web. 10 August 2011. ¡http://www.mathworks.com/help/toolbox/physmod/powersys/ug/f4-23133.html¿

[14] Prakash, Rajiva; , "Robust Control of an Induction Motor Drive with Lyapunov Filter and Linear Quadratic Regulator," *American Control Conference, 1992* , vol., no., pp.1725-1731, 24-26 June 1992

[15] Raumer, Thomas Von, Jean Michel Dion, and Jean Luc Thomas. "Applied Nonlinear Control of an Induction Motor Using Digital Signal Processing." *IEEE Transactions on Control Systems Technology* 2.4 (1994): 327-35. Print.

[16] Vas, Peter. "The Space Phasor Model of A.c. Machines." *Vector Control of AC Machines*. New York : Oxford, Angleterre: Oxford UP, Clarendon., 1990. 5+. Print.

[17] Wang Chenchen; Li Yongdong; , "A novel speed sensorless field-oriented control scheme of IM Using Extended kalman filter with load torque observer," *Applied Power Electronics Conference and Exposition, 2008. APEC 2008. Twenty-Third Annual IEEE* , vol., no., pp.1796-1802, 24-28 Feb. 2008 doi: 10.1109/APEC.2008.4522970

[18] Yau-Tze Kao; Tian-Hua Liu; Chang-Huan Liu; , "Design of H2 and H8 controllers for induction motor drives," *Decision and Control, 1990., Proceedings of the 29th IEEE Conference on* , vol., no., pp.3345-3346 vol.6, 5-7 Dec 1990 doi: 10.1109/CDC.1990.203414

[19] Z. Zhang and J.S. Freudenberg, "On discrete-time loop transfer recovery," in *Proc. Amer. Contr. Conf.*, June 1991.

[20] Zhou, Kemin, and John Comstock. Doyle. "Performance Specifications and Limitations." *Essentials of Robust Control*. Upper Saddle River, NJ: Prentice Hall, 1998. 81+. Print.

APPENDIX:PROGRAM

Following is the matlab program for computing the controller:

```matlab
1  %LQG Controller Design
2  % for the Motor Model
3  % Author: Girish Yajurvedi
4  % Reference: Gu Guoxiang."Design of Feedback Control System." ...
       Discrete-Time Lin-
5  % ear Systems-Theory and Design with applications. To be ...
       published by
6  % Springer, 2011.
7
8  clear
9  ts=5/(1e4);          %1/(25e6);  %%Sampling Time
10 row=1.25678731;              %row for the feedback X
11
12 %Induction Motor Model
13 Lm=0.2459;     Lr=Lm+0.0109; Ls=Lm+0.0073; Rr=5.6885; Rs=5.83; ...
       k1=Lm^2-Ls*Lr; Jeq=55.55/3590; wo=364;
14 A=[Rs*Lr -wo*Lm^2 -Rr*Lm -wo*Lm*Lr;....
15     wo*Lm^2 Rs*Lr wo*Lm*Lr -Rr*Lm;.....
16     -Rs*Lm wo*Lm*Lr Rr*Ls wo*Lr*Ls;....
17     -wo*Lm*Ls -Rs*Lm -wo*Lr*Ls Rr*Ls ]/k1;
18 B=[-Lr 0; 0 -Lr; Lm 0; 0 Lm]/k1; C=[1 0 0 0 ; 0 1 0 0 ]; D=[0 0;0 0];
19 G=ss(A,B,C,D);
20 Gd=c2d(G,ts);
21 [ad,bd,cd,dd]=ssdata(Gd);
22
23 %Adding the weighting function
24 s=tf([1 0],[0 1]);
25 W=3.5*[(s+ 350)/(s ) 0;  0 (s+350 )/(s ) ];
26 [ah,bh,ch,dh]=ssdata(W);
27 Aw=[ah zeros(2,4);B*ch A]; Bw=[bh;B*dh]; Cw=[D*ch C]; Dw=[0 0;0 0];
28 Gw=ss(Aw,Bw,Cw,Dw); Gwd=c2d(Gw,ts);
29 [awd,bwd,cwd,dwd,ts]=ssdata(Gwd); % weighted plant
30
31 % frequency response comparison of weighted and non weighted plant
32 figure(1)
33 sigma(Gd,'r--',Gwd,'b',{1,10000}), grid legend( '\sigma(Gd) ...
       Actual plant ', '\sigma(Gwd) Weighted Plant');
34
35 % Ricatti equations for feedback and estimator design
36 [X,La,Ga]=DARE(awd,bwd,row*cwd'*cwd, eye(2));
```

68

```matlab
37  Y=DARE(awd',cwd', 1000*bwd*bwd', eye(2));
38  omega = eye(2)+bwd'*X*bwd;
39  [uo,so,vo]=svd(omega);
40  omegaf=uo*diag(sqrt(1./diag(so)))*uo';
41  F1=-inv(eye(2)+bwd'*X*bwd)*bwd'*X;
42  F=F1*awd;
43  L=-awd*Y*cwd'*(eye(2)+cwd*Y*cwd')^-1;
44  %L=-awd*bwd*(cwd*bwd)^-1;
45  L0=F1*L;
46  %L0=zeros(2,2);
47
48  % Plant Controller state space equation
49  ak=awd+bwd*F+L*cwd+bwd*L0*cwd; bk=L+bwd*L0; ck=(F+L0*cwd); dk=-L0;
50  k=ss(ak,bk,ck,dk,ts);
51
52  %feedforward part for the closed loop implementation
53  %Considering k(z)=v(z)^-1u(z) left coprime factorization of the ...
        controller
54  av=awd+L*cwd; bv=-bwd; cv=(F+L0*cwd); dv=eye(2);
55  v=ss(av,bv,cv,dv,ts);
56  Vinv=ss(awd+L*cwd+bwd*F+bwd*L0*cwd, bwd,(F+L0*cwd), eye(2),ts);
57  [avin,bvin,cvin,dvin]=ssdata(Vinv);
58  au=awd+L*cwd; bu=L; cu=F+L0*cwd; du=L0;
59  u=ss(au,bu,cu,du,ts);
60
61  %closed loop system state space equation;
62  Acl=[awd-bwd*dv^-1*du*cwd    bwd*dv^-1*ck; bv*dv^-1*du*cwd-bu*cwd ...
         ak-bv*dv^-1*ck];
63  Bcl=[bwd*dv^-1; -bv*dv^-1]*inv(omegaf); Ccl=[cwd zeros(2,6)]; ...
      Dcl=zeros(2,2);
64  Gcl=ss(Acl,Bcl,Ccl,Dcl,ts);
65  Scl=eye(2)-(Gcl);  %% Sensitivity function of the Closed loop plant
66
67  %Close Loop responses
68  figure(2)
69  subplot(2,2,1), dstep(Acl,Bcl(:,1),Ccl(1,:),0,1,200), grid;
70  subplot (2,2,2), dstep(Acl, Bcl(:,2),Ccl(1,:),0,1,200),grid;
71  subplot (2,2,3),  dstep(Acl, Bcl(:,1),Ccl(2,:),0,1,200),grid;
72  subplot (2,2,4),  dstep(Acl, Bcl(:,2),Ccl(2,:),0,1,200),grid;
73
74  figure(3)
75  sigma(Gcl,Scl,{1,100000}),grid
76  legend('\sigma(Gcl) closed loop frequency response','\sigma(Scl) ...
      Closed loop singular values of sensitivity function')
```

69

VITA

Girish Yajurvedi was born in September, 1985, in Baroda, Gujarat, India. He graduated with his Bachelor of Engineering in Electrical engineering from Maharaja Sayajirao University of Baroda, India in 2007. He is presently enrolled in Masters program in electrical and computer engineering at Louisiana State University and is expected to graduate in December 2011. His research interests include Control Theory, Signal Processing and Automation.